




Cite this: *Food Funct.*, 2026, 17, 4464

Plant-protein stabilized emulsions as β -carotene delivery systems: colloidal stability and behaviour during *in vitro* digestion conditions

 Mohsen Ramezani, ^{a,b} Marga Amengual Ramon,^a Laura Salvia-Trujillo ^{a,b} and Olga Martín-Belloso ^{*a,b}

Plant proteins offer a promising clean-label alternative to synthetic surfactants, but their emulsifying properties are strongly dictated by pH. This study investigates how pH (3.0 and 7.0) governs the physico-chemical stability, *in vitro* lipid digestion, and β -carotene bioaccessibility in emulsions stabilized by wheat, pea, and soy proteins, benchmarked against a Tween 80 nanoemulsion. Interfacial tension analysis confirmed Tween 80's superior performance (reaching 2.3 mN m⁻¹ at pH 3.0 and 1.7 mN m⁻¹ at pH 7.0). Among the proteins, wheat was most effective, and all proteins showed higher activity at pH 7.0 (2.4–2.8 mN m⁻¹) than at pH 3.0 (3.3–4.2 mN m⁻¹). In terms of colloidal stability, at both pH levels the Tween 80 nanoemulsion remained stable with a consistent size of ~0.2 μ m. At pH 3.0, wheat protein emulsions were highly stable, forming fine droplets (0.42 μ m) and increased electrostatic repulsion (+15 mV). Conversely, soy and pea emulsions were unstable at pH 3.0 (droplets >6 μ m) but stabilized at neutral pH, where wheat emulsions destabilized (droplets >7 μ m). The small size of the Tween 80 nanoemulsion enabled the fastest (24.5%/min^{0.5}) and most complete (79.5%) lipid digestion, while protein emulsions digested slower. Notably, wheat protein emulsions at pH 3.0 achieved a superior β -carotene bioaccessibility (14.5%), comparable to the Tween 80 nanoemulsion (12.5%). This performance was attributed to efficient proteolysis and micelle formation. Soy and pea proteins had lower bioaccessibility (8–10%). These findings show that wheat protein at acidic pH is a promising clean-label strategy for enhancing both emulsion stability and nutrient bioaccessibility.

Received 18th December 2025,
Accepted 23rd April 2026

DOI: 10.1039/d5fo05533d

rsc.li/food-function

1. Introduction

β -Carotene is a carotenoid widely present in fruits and vegetables, known for its potential health benefits such as reducing the risk of certain cancers, cardiovascular diseases, and age-related macular degeneration.¹ Despite these benefits, the integration of β -carotene into functional foods and nutraceutical products faces significant challenges due to its inherent instability and poor solubility in aqueous media. Factors such as exposure to oxygen, heat, light, and acidic environments significantly diminish its bioactivity and bioavailability.² This degradation is particularly pronounced during food processing, storage, and gastrointestinal digestion.³ Moreover, its low water solubility further complicates its incorporation into aqueous-based food systems.⁴ To address these limitations,

various encapsulation techniques as delivery systems have been explored to enhance β -carotene's stability and bioavailability. Among these, oil-in-water (o/w) emulsions, have gained considerable attention due to their ease of preparation, scalability, and cost-effectiveness, making them suitable vehicles for lipophilic bioactives.⁵

The global food and nutraceutical markets are undergoing a significant transformation driven by consumer demand for "clean-label" products, which are perceived as more natural and healthier. This trend has created a pressing need to replace synthetic additives, such as the widely used non-ionic surfactant Tween 80, by functional plant-based alternatives.^{6,7} Plant proteins, sourced from abundant crops like wheat, soy, and pea, have been identified as leading candidates for this role due to their natural origin, nutritional benefits, and inherent amphiphilicity, which allows them to stabilize oil-in-water emulsions.⁸ Plant proteins are especially appealing emulsifiers because of their biocompatibility, sustainability, and capacity to encapsulate and deliver bioactive compounds effectively.^{7,9}

Current research suggests that while plant proteins are good natural emulsifiers, they often need to be combined with

^aDepartment of Food Technology, Engineering and Science, University of Lleida, Av. Alcalde Rovira Roure 191, 25198 Lleida, Spain. E-mail: mohsen.ramezani@udl.cat, mar35@alumnos.udl.cat, laura.salvia@udl.cat, olga.martin@udl.cat; Tel: (+34) 973702593

^bAgrotecnio Center, Av. Alcalde Rovira Roure 191, 25198 Lleida, Spain



other ingredients to effectively protect sensitive nutrients like β -carotene. To achieve this, previous studies have largely focused on two major approaches: physical complexation and chemical or metal-ion coordination.

Physical approaches, such as protein-polysaccharide complexes and multilayer interfacial assembly, typically involve layering plant proteins with carbohydrates or natural surfactants.^{10,11} The primary advantage of this strategy is the creation of a thick, firm physical barrier that excellently prevents oil droplets from coalescing, thereby improving structural stability.¹⁰ However, a major limitation is that these thick shells can impede the action of digestive enzymes. For instance, while some pectin-coated systems allow for moderate digestion,¹¹ dense multi-layered coatings (e.g., zein, alginate, and rhamnolipid) can protect the oil so effectively that they significantly slow down lipid digestion, which hinders the immediate bioaccessibility and absorption of β -carotene.¹²

In contrast, chemical modifications and metal-ion coordination focus on tightening the interfacial layer rather than just thickening it. Techniques that create covalent bonds between proteins and antioxidants,¹³ or utilize metal ions (like iron) to cross-link proteins and polyphenols,¹⁴ offer distinct advantages. These methods form dense, highly cohesive shields that strongly resist environmental degradation while maintaining excellent nutrient release, achieving higher β -carotene bioaccessibility (up to 46.5%) compared to physical mixtures.^{13,14} While highly effective, the limitation of these complex modification methods alongside other treatments like heating,¹⁵ irradiation,¹⁶ sonication,¹⁷ hydrolysis,¹⁸ oxidation,¹⁹ and pH-shifting²⁰ is that they often complicate food processing and drift away from the simplicity desired in clean-label formulations.²¹

Consequently, a significant knowledge gap remains. Much of the current literature focuses heavily on adding complex ingredients or utilizing intensive modifications to overcome the inconsistent performance of plant-protein emulsions. However, fundamental studies on how the food matrix's most basic intrinsic property such as environmental pH directly governs the performance of these delivery systems are limited. Despite the general understanding that pH modulates protein conformation and charge,^{22,23} it remains entirely unclear how the intrinsic pH of a simple, unmodified plant-protein emulsion impacts the ultimate biological fate of the encapsulated bioactive. There is a lack of systematic investigation directly linking the pH-dictated electrostatic charge of different proteins in the aqueous phase to subsequent lipid digestion kinetics and nutrient bioaccessibility, which is the true measure of a delivery system's success.

The influence of pH on protein structure and function is a cornerstone of protein science.²⁴ It is well-established that pH modulates a protein's net surface charge, governed by the protonation state of its acidic and basic amino acid residues.²² Consequently, at pH values distant from a protein's isoelectric point (pI), increased electrostatic repulsion enhances solubility and promotes the formation of a stable, charged layer at

the oil-water interface, which is critical for preventing droplet coalescence.^{24,25} Conversely, near the pI, reduced charge leads to protein aggregation and poor emulsifying performance.²⁶ Furthermore, pH can induce conformational changes, causing proteins to partially unfold.²⁴ This unfolding can expose buried hydrophobic regions, which may enhance the protein's ability to adsorb to the oil interface, but can also lead to irreversible aggregation if not properly controlled.²⁷ Previous studies have extensively characterized these pH-dependent changes in solubility,²⁸ surface hydrophobicity,²⁶ and interfacial rheology²⁴ for various plant proteins.

While these relationships between pH and the physico-chemical aspects of emulsion formation are well-documented, we hypothesize that these pH-governed interfacial properties have direct and predictable consequences for the biological performance of the emulsion as a delivery system. Specifically, we propose that the formation of a stable, highly-charged interfacial layer under optimal pH conditions does not only prevent physical destabilization but also critically mediates the accessibility of the lipid core to digestive enzymes, thereby controlling lipolysis kinetics and the subsequent bioaccessibility of encapsulated nutrients.

Therefore, this study aims to systematically test this hypothesis by evaluating the emulsifying properties of wheat, pea, and soy protein isolates within two distinct pH environments. β -Carotene-loaded emulsions at pH 7.0 (representing neutral foods) and pH 3.0 (representing acidic foods) were prepared and characterized. These conditions were strategically chosen to create distinct charge profiles for each protein based on their known isoelectric points, allowing for a clear assessment of how they would behave under different scenarios. The investigation will comprehensively link fundamental interfacial properties and emulsion stability metrics to functional outcomes, namely *in vitro* lipid digestion kinetics and β -carotene bioaccessibility. By benchmarking these systems against a conventional Tween 80 nanoemulsion, this work will elucidate how environmental pH can be understood and leveraged to formulate highly effective, clean-label delivery systems for lipophilic bioactives.

2. Materials and methods

2.1 Materials

Pea protein isolate (82.9% protein, 3.5% moisture, Profam, Lot E2104907B1), soy protein isolate (95.2% protein, 3.0% moisture, 0.4% oil, Profam 974, Lot 22012011), and wheat protein isolate (89.0% protein, 6.0% moisture, 0.6% fat, 0.9% ash, Prolite MeatTex, Lot 223-16) were all generously provided by ADM (Netherlands, manufactured in the USA). Refined corn oil was sourced from Deoleo Global, S.A.U. (Córdoba, Spain). Polyoxyethylene (80) sorbitan monooleate (Tween 80) was acquired from Panreac (Barcelona, Spain). β -Carotene, porcine pepsin (77160), dried unfractionated bovine bile (B3883), pancreatine (≥ 3 USP, P1625), HCl, NaOH, $\text{CaCl}_2(\text{H}_2\text{O})_2$, $(\text{NH}_4)_2\text{CO}_3$, NaCl, KH_2PO_4 , CH_3COOH , CH_3COONa and $\text{MgCl}_2(\text{H}_2\text{O})_6$ were purchased from Sigma Aldrich (St. Louis,



USA). KCl was obtained from Panreac (Barcelona, Spain). Ethanol with 99.9% purity from Fisher Chemical, Thermo Fisher Scientific (Leicestershire, UK), and hexane with >95% purity from Scharlau, Scharlab S.L. (Barcelona, Spain) were used in this study. Ultrapure water (Synergy® UV, Millipore, France) was used for all analyses.

2.2 Methods

2.2.1 Protein slurries preparation. Protein slurries (0.4% w/w) of pea, soy, and wheat proteins were prepared by overnight hydration in pH 3.0 (acetate buffer) or pH 7.0 (phosphate buffer) with gentle magnetic stirring. To avoid clumping, protein powder was gradually added to the stirring buffer. These slurries served as the basis for preparing the emulsifiers and were also used for further analyses.

2.2.1.1 Dynamic interfacial tension (DIFT) of the protein slurries and Tween 80 solution. To investigate protein adsorption at the oil/water interface, DIFT was measured using a Kruss DSA 25 Drop Shape Analyzer (Krüss, Germany) with the inverted pendant drop method, following the procedure outlined by Velderrain-Rodríguez *et al.*²⁹ with slight modifications. Aqueous solutions of surfactants (0.1% w/w Tween 80, wheat, pea, and soy protein isolates) were prepared in buffers at pH 3.0 and pH 7.0 overnight. These solutions were placed in a glass cuvette, and a high-speed camera recorded the profile of an oil droplet immediately after its formation from a J-shaped needle (0.5 mm) submerged in the solution. IFT was calculated using the simplified Young-Laplace equation:

$$\sigma = \frac{RP_c}{2} \quad (1)$$

where ' σ ' is the surface tension being a force that acts at the interface between oil and water, tending to minimize the surface area (N m^{-1}), ' R ' is the experimental radius of the curved surface of the oil droplet (m). In our case where the interface is spherical, ' R ' represents the radius of that spherical surface, and ' P_c ' represents the pressure difference across the curved interface (Pa), which is also known as capillary pressure: the difference between the pressure inside the droplet and the pressure outside. This formula enables the quantification of the time-dependent deformation experienced by the oil droplet. Droplet deformation over time, quantified by IFT, reflects the emulsifiers' ability to adsorb to the oil/water interface.

To assess the early-stage adsorption kinetics at the oil-water interface, the initial 10 minutes of interfacial tension (mN m^{-1}) was plotted against the square root of time (\sqrt{t} , in $\text{min}^{0.5}$).³⁰ The initial slope of the linear region of the γ vs. \sqrt{t} curve was determined for each emulsifier using linear regression. The resulting slope (k) was expressed in $\text{mN m}^{-1} \text{min}^{-0.5}$ and interpreted as the interfacial tension decay rate, representing the rate at which surface-active molecules adsorbed to the interface under diffusion-controlled conditions. Higher absolute values of k indicate a more rapid decrease in interfacial tension, suggesting faster initial interfacial activity.

2.2.2 Emulsion preparation

2.2.2.1 Corn oil enrichment with β -carotene. A 0.1% (w/w) β -carotene solution in corn oil was prepared by heating the mixture at 50 °C with continuous stirring for 15 minutes. This concentration is well below the reported maximum solubility of β -carotene in corn oil ($0.41\% \pm 0.01\%$),³¹ ensuring that the carotenoid remains molecularly dispersed in the lipid phase without recrystallization [sink condition]. The mixing was followed by a one-minute ultrasound treatment using an ultrasonic probe (UP400S, Hielscher Ultrasonics GmbH, Teltow, Germany) operating at 0.5 cycle, 24 kHz and 50% amplitude to disperse any β -carotene aggregates and another 15 minutes of stirring at 50 °C to ensure complete dissolution.³² The container was covered with aluminium foil throughout the process to minimize light-induced degradation of β -carotene.

2.2.2.2 Emulsions and nanoemulsions preparation. Emulsions and nanoemulsions were prepared using an aqueous phase consisting of pea, wheat, or soy protein, pre-stirred overnight in buffers at pH 3.0 or pH 7.0 (section 2.2.1). A control nanoemulsion was formulated using Tween 80 as the emulsifier. All formulations had a surfactant-to-oil ratio (SOR) of 0.1. Initially, coarse emulsions were produced by mixing a 4% lipid phase (enriched with β -carotene) and a 96% aqueous phase.⁵ An oil phase concentration of 4% (w/w) was selected for three primary reasons. First, it represents a model dilute functional beverage system. Second, it prevents high viscosity from interfering with the microfluidization process. Finally, and crucially for the subsequent *in vitro* digestion assays, a 4% lipid fraction provides an optimal substrate-to-enzyme ratio. In standard digestion models, high oil concentrations can lead to the saturation of pancreatic lipase, artificially limiting lipolysis and masking the true effect of the interfacial layer.^{33,34} Conversely, highly dilute systems digest too rapidly to capture distinct kinetic profiles. The 4% oil fraction ensures that enzyme availability is not the limiting factor, allowing us to accurately isolate and evaluate how the different pH-governed protein interfaces impact lipolysis kinetics and β -carotene bioaccessibility. The coarse emulsion was made using an Ultra-Turrax homogenizer (Model T25D, IKA Works, Inc., Staufen, Germany) at 7200 rpm for 3 minutes. These coarse emulsions were then passed through a microfluidizer (MP-110, Microfluidics Corp., Westwood, MA, USA) at 100 MPa for 3 cycles to produce the final emulsions and nanoemulsions. Freshly prepared emulsions were kept at 25 °C prior to analysis.

2.2.3 *In vitro* lipid digestion. The *in vitro* digestion procedure, adapted from Ramezani *et al.*³⁵ with minor modifications, comprised gastric and intestinal phases. Freshly prepared simulated gastric fluid (SGF) and simulated intestinal fluid (SIF), preheated to 37 °C, were used. SGF contained 100.58 mM KCl, 13.12 mM KH_2PO_4 , 7.29 mM $(\text{NH}_4)_2\text{CO}_3$, 1052.48 mM NaCl, 1.75 mM $\text{MgCl}_2(\text{H}_2\text{O})$ in ultrapure water. SIF contained 10 mM CaCl_2 and 160 mM NaCl.

The emulsion dose and digestive fluid volumes were selected to reflect physiologically relevant adult human gastro-



intestinal conditions, following the standardized INFOGEST 2.0-based protocol.³³ *In vitro* gastric digestion procedures commonly use a 1 : 1 meal-to-digestive fluid ratio, which mimics the fed-state gastrointestinal environment while allowing feasible reactor volumes in the laboratory.^{33,36}

The oral phase was omitted as the structured lipid carriers were not expected to undergo significant physicochemical modifications during the brief exposure to simulated salivary conditions.³⁷ The amount of initial material introduced into the gastric phase was adjusted for each sample based on its lipid content to ensure a standardized delivery of 0.25 g of oil.³⁸

According to previous reports, extensive lipolysis in high-fat systems is governed by lower lipid-to-lipase ratio.^{33,39} Therefore, near-complete digestion can be achieved either by increasing the lipase concentration or by diluting the lipid phase. To maintain the physiological relevance of the enzyme concentrations as defined in the INFOGEST protocol, the latter approach was adopted. Diluting the lipid system ensured that the lipase-to-substrate ratio was not a limiting factor, thereby facilitating near-complete lipid digestion. Accordingly, for the gastric phase, 6.25 g of each emulsion or nanoemulsion (containing 0.25 g of oil) was first diluted with 13.75 mL of Milli-Q water to reach a standardized sample mass of 20 g. Subsequently, this diluted sample was mixed with SGF in a 1 : 1 (w/w) ratio by adding 20 mL of gastric reagents. These reagents consisted of 18.2 mL of pepsin solution (8.8 mg mL⁻¹ in SGF), 10 μ L of 0.3 M CaCl₂, and 1.39 mL of Milli-Q water. To strictly adjust the pH to 3.0, a variable volume of 1N HCl (maximum \sim 0.4 mL) was added; this concentration was selected to minimize the dilution effect, resulting in a final reaction volume of 40 mL. The flasks were covered with aluminium foil and incubated in a digital opaque incubator chamber (I10-OE, OVAN, Spain) at 37 °C and 100 rpm for 2 hours.

For the intestinal phase, 30 g of chyme from the gastric phase was combined with 3.5 mL of preheated bile salt solution (54 mg mL⁻¹ in pH 7.0 phosphate buffer), and 1.5 mL of preheated SIF. The pH was adjusted to 7.0 with 1 M NaOH, and the intestinal phase was initiated by adding 2.5 mL of pancreatin solution (124 mg mL⁻¹ in pH 7.0 phosphate buffer). The mixture was stirred at 37 °C for 2 hours, and the release of free fatty acids (FFAs) was monitored using a pH-STAT (Titrand 902, Metrohm, Switzerland) with TIAMO 2.5 software.

2.2.4 Physicochemical characterization of initial and digested emulsions and nanoemulsions

2.2.4.1 Particle size. Particle size was analysed using different instruments depending on the sample. Initial nanoemulsions stabilized with Tween 80 (diluted 1 : 1000 ultrapure water) were measured with a Zetasizer NanoZS (Malvern Instruments Ltd, Worcestershire, UK). For initial emulsions stabilized with proteins, as well as digested emulsions and nanoemulsions after the gastric and intestinal phases, a Mastersizer 3000 (Malvern Instruments Ltd, Worcestershire, UK) was used due to the larger particle sizes. Results are

reported as the volume mean diameter (d_{32}). Measurements were performed at 25 °C using a refractive index of 1.466 for corn oil. Samples were dispersed in ultrapure water to reach an obscuration level between 4% and 8%, with stirring at 1800 rpm using a Hydro SM dispersion unit (Malvern Instruments Ltd).

2.2.4.2 Microstructure. The microstructure of emulsions and nanoemulsions, both before and after each stage of simulated gastrointestinal digestion, was examined using an Olympus FV1000 confocal microscope (Melville, NY) with a \times 100 objective lens. Samples (approximately 1 μ L) were placed on microscope slides and covered with coverslips. Images were processed and analysed using the Olympus FV10-ASW viewer software.

2.2.4.3 Particle charge. Particle charge (zeta potential) was measured before and after each stage of simulated digestion using a Zetasizer NanoZS (Malvern Instruments Ltd, Worcestershire, UK). Samples were diluted 1 : 1000 in Milli-Q water and placed in a microelectrophoretic capillary cell. The zeta potential was calculated from the electrophoretic mobility using Henry's equation, based on the frequency shift of a laser beam caused by particle movement towards an oppositely charged electrode. The cell temperature was maintained at 25 °C.

2.2.4.4 Dynamic viscosity. Dynamic viscosity of the initial emulsions and nanoemulsions was measured at 25 °C using a SV-10 vibro-viscometer (A&D Company, Tokyo, Japan). The instrument measures viscosity by detecting the resistance of emulsions and nanoemulsions to the vibration of two sensor plates oscillating at 30 Hz with a 0.4 mm amplitude. Measurements were performed on 10 mL aliquots in a dedicated plastic cuvette.

2.2.4.5 Colloidal stability. The stability of initial emulsions and nanoemulsions was evaluated using a Turbiscan MA 2000 optical analyser (Formulation, Toulouse, France). This instrument employs static multiple light scattering to non-destructively identify instability phenomena like flocculation, coalescence, sedimentation, or creaming, detecting these changes well before they become visible to the naked eye. A 7 mL sample was placed in a glass cell and scanned vertically with a near-infrared light beam (800 nm). Due to sample opacity, only backscattered light, detected at a 45° angle, was used for analysis. Backscattering intensity is affected by particle size and volume fraction, with smaller particles scattering more uniformly (Rayleigh scattering), and larger particles scattering more forward (Mie scattering), thus reducing backscattering. Higher volume fractions and multiple scattering in concentrated systems also influence backscattering intensity. Emulsions and nanoemulsions' stability was monitored over a 24 hour period to characterize early physical stability rather than long-term storage behaviour.

2.2.5 Lipid digestibility and β -carotene bioaccessibility

2.2.5.1 Free fatty acid release. The extent of lipid digestion was determined by measuring the volume of NaOH solution needed to neutralize the FFAs released by lipase activity. The



percentage of FFAs released was calculated using the following equation:

$$\% \text{ FFA} = \frac{V_{\text{NaOH}} \times M_{\text{NaOH}} \times \text{Mw}_{\text{lipid}}}{2 \times W_{\text{lipid}}} \quad (2)$$

where V_{NaOH} is the volume of NaOH solution used (L), M_{NaOH} is the molarity of NaOH solution (mol L^{-1}), Mw_{lipid} is the molecular weight of the lipid ($872.24 \text{ g mol}^{-1}$ (ref. 40)), and W_{lipid} is the initial weight of oil in the reaction vessel (g).

For the protein-stabilized emulsion it is acknowledged that some NaOH consumption during the pH-stat assay could be due to protein hydrolysis in addition to lipid hydrolysis. However, given the low and constant protein-to-oil ratio (10% w/w) used, the contribution from proteolysis was considered negligible to simplify calculations. Therefore, all consumed NaOH was attributed to the neutralization of free fatty acids from lipolysis. While this may lead to a slight overestimation of digestion in the protein systems, it does not affect the validity of the comparisons between them or the overall conclusions drawn relative to the Tween 80 benchmark.

2.2.5.2 Kinetics of lipolysis. To determine the transition time between the initial rapid and subsequent slower lipolysis phases, a 45° rotation transformation was applied to the time (t) and FFA percentage data. This yielded rotated coordinates, $t_{\text{rotated}} = (t + \text{FFA})/\sqrt{2}$, and $\text{FFA}_{\text{rotated}} = (\text{FFA} - t)/\sqrt{2}$. The time corresponding to the maximum $\text{FFA}_{\text{rotated}}$ value was identified as the transition time. Each phase was then modelled individually using the equation:

$$\text{FFA}_{(t)} = \text{FFA}_0 + k \cdot t^{0.5} \quad (3)$$

where $\text{FFA}_{(t)}$ is the instantaneous FFAs release at time ' t ' (%), FFA_0 is the initial FFAs release at $t = 0$ (%), k is the rate constant ($\% \text{ min}^{-0.5}$), and t is time during the intestinal digestion process (min). Model's fit was assessed using R^2 and residual plots. Significant differences between estimated parameters for different samples were determined using a 95% confidence interval.

2.2.5.3 β -Carotene bioaccessibility. In this study, the *in vitro* digestion was confirmed for β -carotene to be under sink conditions. The maximum theoretical concentration of β -carotene in the intestinal phase was calculated to be approximately 0.005 mg mL^{-1} ($\sim 9 \mu\text{M}$). This value is well below the reported saturation limit of β -carotene in mixed micelles ($15 \mu\text{L}$), ensuring that the bioaccessibility measurements were not limited by the solubility capacity of the micellar phase.⁴¹

After 120 minutes of *in vitro* intestinal digestion, the digest was centrifuged at 4788g for 30 minutes at 25 °C (Micro 220R, Hettich, Tuttlingen, Germany) to separate the phases. This resulted in a bottom precipitate, a middle clear micellar phase containing bioaccessible β -carotene, and a thin top layer of undigested oil. A 0.5 mL sample of the micellar phase was collected, vortexed with 5 mL of hexane–ethanol (3:2) for 30 seconds, and the β -carotene content in the upper hexane layer was measured spectrophotometrically at 450 nm (UV-VIS spectrophotometer V-670 Jasco, Tokyo, Japan) using a hexane

blank. β -Carotene content was quantified using a standard curve based on hexane. β -Carotene bioaccessibility (%) was calculated as:

$$\beta\text{-Carotene bioaccessibility (\%)} = \frac{C_{\text{micelle}}}{C_{\text{initial emulsion}}} \times 100 \quad (4)$$

where C_{micelle} and $C_{\text{initial emulsion}}$ are the β -carotene concentrations (mg mL^{-1}) in the micellar fraction and the initial emulsion/nanoemulsion, respectively.⁴²

2.2.6 Statistical analysis. All treatments were performed in at least duplicate to ensure reliability. Data normality (Shapiro-Wilk test) and variance homogeneity were checked using JMP Student Edition 18 (SAS Institute Inc.). Due to non-normal data and unequal variances, the Kruskal-Wallis test in RStudio (version 2025.09.1 Build 401) was used to find differences among groups. When significant differences were found, Conover's *post-hoc* test with FDR correction (PMCMRplus package, version 1.9.12) was applied for pairwise comparisons. Significance letters were assigned using the agricolae package (version 1.3.7).

3. Results and discussion

3.1 Protein dynamic interfacial tension (DIFT)

The interfacial characteristics of proteins used as emulsifiers significantly influence lipid digestion, therefore, understanding their stabilization mechanisms is crucial. To examine the role of interfacial properties in lipid digestion, the DIFT at the oil–water interface for Tween 80 (as a benchmark), along with wheat, soy, and pea protein isolates was measured. All emulsifiers reduced IFT, indicating their adsorption to the oil–water interface (Fig. 1). Although the emulsifiers displayed a similar overall pattern of DIFT orders across both pH conditions, their effectiveness in lowering IFT varied significantly.

At both pH, Tween 80 exhibited superior emulsification activity compared to the plant proteins, rapidly reaching a relatively constant IFT (Fig. 1A and B). This suggests that Tween 80, the emulsifier with the lowest molecular weight ($\text{MW} \approx 1.23 \text{ kDa}$, compared to proteins with $\text{MW} \approx 18\text{--}100 \text{ kDa}$), adsorbed more rapidly to the oil–water interface (kinetic constant of interfacial tension decay = $-0.56 \text{ mN m}^{-1} \text{ min}^{-0.5}$, Fig. 1C, $-0.61 \text{ mN m}^{-1} \text{ min}^{-0.5}$, Fig. 1D), leading to faster interface saturation and stabilization of oil droplets, consistent with previous findings.²⁹ The enhanced efficiency of Tween 80 can be attributed to a dual effect: its lower molecular weight promotes a higher diffusion rate, while its smaller molecular size enables a denser packing of amphiphilic molecules at the interface, resulting in more effective reduction of IFT.^{43,44} Moreover, the longer times required for proteins' surface denaturation, a process involving conformational rearrangement of proteins upon adsorption at the oil–water interface, may further limit their efficiency in reducing IFT compared to Tween 80.^{44,45}

At pH 3.0, wheat protein was the most effective in reducing the IFT (Fig. 1A). Soy and pea proteins showed similar behaviour, reaching final IFT values of 3.9 mN m^{-1} and 4.2 mN m^{-1} ,



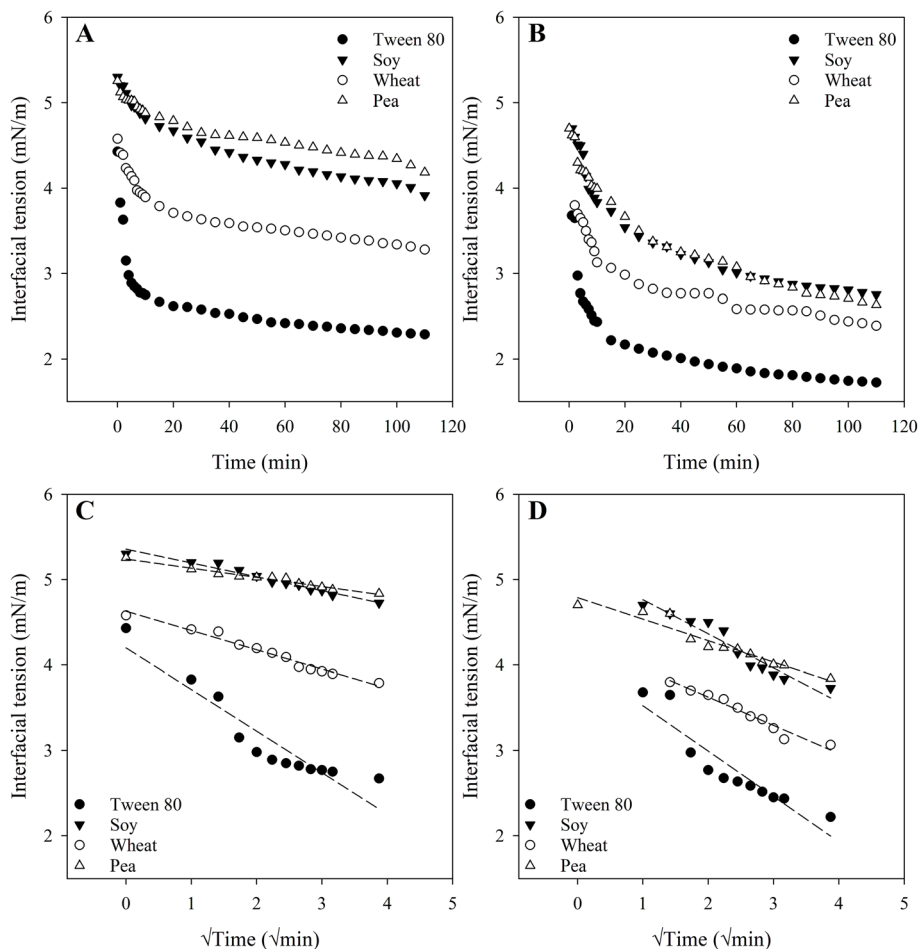


Fig. 1 Interfacial tension (mN m^{-1}) over time (min) for Tween 80 ●, soy ▼, wheat ○ and pea △ protein isolates (0.04% w/w) at (A) pH 3.0 or (B) pH 7.0. Early-stage adsorption kinetics at (C) pH 3.0 or (D) pH 7.0.

respectively, after two hours, while wheat protein exhibited an intermediate IFT value between the Tween 80 and other proteins, lowering the IFT to 3.2 mN m^{-1} . The interfacial tension of the protein-laden interface is hypothesized to be influenced by conformation or flexibility of the proteins and the surface hydrophobicity.⁴⁶ Soy and pea proteins are globular proteins dominated by β -sheet-type secondary structures (hard proteins), whereas wheat gluten (soft protein) is considered an irregular plant protein.^{46,47} Globular proteins are less flexible and require more time to align to the interface.⁴⁸ Therefore, greater conformational rearrangement of wheat proteins compared to soy and pea proteins can be expected during their adsorption at the interface. Moreover, wheat proteins are inherently hydrophobic, whereas soy and pea proteins exhibit greater water solubility.⁸ A negative correlation is often observed between surface hydrophobicity and interfacial tension.⁴⁶ Proteins with higher surface hydrophobicity tend to adsorb more rapidly at the oil-water interface due to the stronger affinity of their hydrophobic residues for the oil phase. This enhanced interfacial activity facilitates quicker molecular reorientation and packing at the interface, ultimately resulting in a faster and more substantial reduction in interfacial

tension.⁴⁶ The kinetic constants of interfacial tension decay further support this observation, where soy and pea proteins exhibited kinetic constants of $-0.16 \text{ mN m}^{-1} \text{ min}^{-0.5}$ and $-0.11 \text{ mN m}^{-1} \text{ min}^{-0.5}$, respectively, whereas wheat protein displayed an intermediate rate of $-0.23 \text{ mN m}^{-1} \text{ min}^{-0.5}$.

However, at pH 7.0 (Fig. 1B), all emulsifiers exhibited greater reductions in IFT compared to their respective behaviour at pH 3.0 (Fig. 1A). At pH 7.0, the final IFT values after two hours were 1.72 mN m^{-1} (Tween 80), 2.39 mN m^{-1} (wheat), 2.75 mN m^{-1} (soy), and 2.63 mN m^{-1} (pea). This reduced IFT indicated enhanced interfacial activity, which is likely due to the improved ability of the emulsifiers to adsorb at the interface and undergo structural rearrangements.²⁴ This observation is consistent with Shimizu *et al.*,⁴⁹ who found that the more rigid and denaturation-resistant conformation of β -lactoglobulin at pH 3.0 compared to pH 7.0 led to reduced emulsifying and surface activity at acidic pH. Aluko and colleagues also found that at a pH of 7.0, the foaming ability of pea and soy protein isolates increased compared to at pH 3.0.⁵⁰ This improvement was attributed to a higher net charge density at pH 7.0, which enhanced protein unfolding and flexibility, thereby promoting the formation of a stable interfacial film. Zhou *et al.*²⁴ also reported that wheat



protein exhibited a greater ability to reduce interfacial tension at alkaline pH compared to acidic pH. This was attributed to the alkaline shift which enhanced the proteins' adsorption kinetics, thereby facilitating faster and more effective diffusion to the oil-water interface. As reported by Gharsallaoui *et al.*,⁵¹ while pea proteins adsorbed more rapidly at pH 7.0 than under acidic conditions (pH 2.4), the resulting interfacial films were weak and inhomogeneous. In contrast, the films formed under acidic conditions were thicker and possessed superior elastic properties, which yielded more stable emulsions. This finding underscores that the quality and rheological properties of the interfacial film, rather than simply the rate of protein adsorption, are the primary determinants of colloidal stability. Nevertheless, higher kinetic constant of interfacial tension decay were also observed for all emulsifiers at pH 7.0, with values $-0.36 \text{ mN m}^{-1} \text{ min}^{-0.5}$ (wheat), $-0.44 \text{ mN m}^{-1} \text{ min}^{-0.5}$ (soy), and $-0.26 \text{ mN m}^{-1} \text{ min}^{-0.5}$ (pea), further supporting the improved adsorption kinetics under neutral conditions (Fig. 1D).

3.2 Emulsion formation and emulsion stabilization capacity of plant-proteins

3.2.1 Particle size and microstructural organization. The particle size distribution and microstructure of all initial oil-in-water (o/w) emulsions and nanoemulsions were analysed to understand the structural organization of lipids within them. These characteristics are critical factors that likely influence the digestion kinetics of these systems.

At both pH levels, only Tween 80 formed nanoemulsions with nanometric droplet sizes (Fig. 2) consistent with previous studies.^{42,52} At pH 3.0, it formed a nanoemulsion with an average particle size of $0.18 \mu\text{m}$, whereas at pH 7.0, the nanoemulsion had an average particle size of $0.21 \mu\text{m}$. Microscopic images confirmed the presence of sub-micron oil droplets in these Tween 80-based nanoemulsions (Fig. 2).

At pH 3.0, the wheat protein-based emulsion also exhibited size within the nanometre range ($0.42 \pm 0.10 \mu\text{m}$). As previously discussed (section 3.1), wheat protein exhibited a greater ability to adsorb to the interface compared to the other proteins. This likely contributed to its efficient coverage of oil droplets during microfluidization and enhanced protection against coalescence, resulting in smaller particle size. However, the particle size distribution of wheat protein at pH 3.0 was smaller than at pH 7.0, with an average particle size of $7.33 \pm 0.27 \mu\text{m}$ at pH 7.0. Given that flocculation was not observed, the larger droplet sizes detected at the higher pH 7.0 must be attributed to enhanced coalescence, an observation visually confirmed by the micrographs (Fig. 2). This suggests a coalescence-dominated emulsification process, which is typical for emulsifiers with slow adsorption kinetics.⁵³ During homogenization, newly formed droplets must be stabilized immediately to prevent them from coalescing. If the emulsifier's adsorption to the interface is too slow, this rapid stabilization fails, leading to larger final droplet sizes. Therefore, it can be inferred that at pH 7.0, the lower solubility and functionality of wheat proteins resulted in slower adsorption kinetics, making them less effective at stabilizing

the oil droplets formed during homogenization. This outcome seemingly contradicts the IFT results (section 3.1), which indicated better interfacial activity for wheat protein at pH 7.0. This discrepancy can be explained by two key differences between the emulsification process and the IFT measurement. First, the high-pressure microfluidization used for emulsification can induce protein denaturation, exposing more hydrophobic sites and altering emulsifying properties, whereas the IFT measurement assesses proteins in their native state.⁵³ Second, the apparently superior interfacial activity at pH 7.0 in the IFT test could be an artifact of protein solubility. Wheat proteins exhibit lower solubility at pH 7.0, which is closer to their isoelectric point.⁵³ In the IFT measurement setup, an oil droplet is placed at the bottom of the container. It is probable that the less soluble proteins at pH 7.0 precipitate more rapidly, settling downwards and accumulating at the oil-water interface more quickly than the highly soluble proteins at pH 3.0. This would result in a faster and more significant reduction in the measured IFT, without necessarily reflecting a better ability to form a stable emulsion under dynamic conditions. In fact, Liang and Tang⁵⁴ found that insoluble proteins can also adsorb at an interface, where they tend to form a significantly thicker interfacial film compared to their soluble counterparts.

In contrast to the emulsion stabilized with wheat protein, emulsions stabilized by soy and pea proteins displayed larger particle size distribution at pH 3.0 compared to pH 7.0. This observation aligns with the findings of Franco *et al.*⁵⁵ who reported that pea protein-stabilized emulsions exhibited consistently larger particle size distributions at lower pH values (pH 3.5) compared to pH 7.0. The authors attributed this to the higher adsorption kinetics of pea proteins at higher pH, which facilitated more effective coverage of the oil-water interface (consistent with section 3.1 and Fig. 1), thereby preventing droplet coalescence. This can also be attributed to the isoelectric points of these plant proteins. Pea and soy proteins have isoelectric points around pH 4.0–6.0 and 4.0–5.0, respectively, while wheat proteins have isoelectric point around pH 6.0–7.0.⁵⁶ Near their isoelectric points, proteins exhibit reduced electrostatic repulsions, leading to increased aggregation and larger particle sizes.⁵⁷ Furthermore, the neutrality of proteins at or near their isoelectric points reduces their tendency to coat oil droplets effectively resulting in larger or coalesced oil droplets, as observed in the microscopic images of the initial emulsions at pH 3.0 (Fig. 2).

3.2.2 Particle charge. Zeta potential, defined as the electric potential at a particle's slipping plane in a solution, is a crucial parameter for understanding the stability of colloidal dispersions.⁵⁸ It reflects the magnitude of electrostatic repulsion or attraction between particles. For orally administered emulsions and nanoemulsions, zeta potential significantly influences their ability to overcome physiological barriers and facilitates the systemic absorption of encapsulated active agents.⁵⁹ Factors such as pH, ionic strength, and the presence of adsorbed molecules or surfactants can all affect zeta potential.⁶⁰



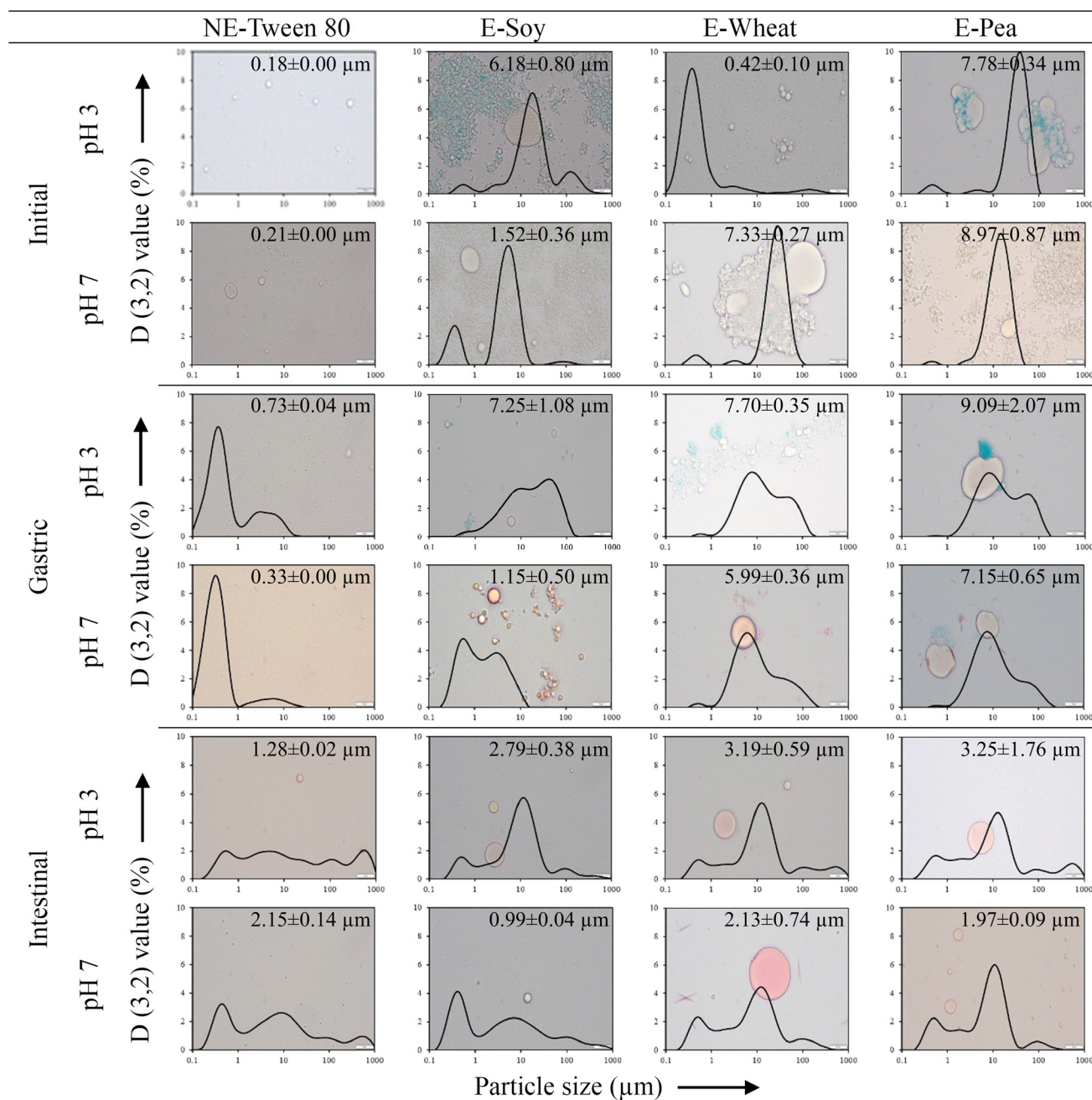


Fig. 2 Micrographs and particle size distributions of initial nanoemulsions (NE) and emulsions (E), their corresponding chyme, and digests. Formulations were stabilized by Tween 80 (NE-Tween 80), soy (E-Soy), wheat (E-Wheat), or pea (E-Pea) protein isolates. Scale bars = 10 μm.

In this study, the changes in the electrical characteristics (zeta potential) of the initial emulsions and nanoemulsions were investigated to evaluate their potential impact on *in vitro* lipid digestion (Fig. 3). Among the various formulations, the nanoemulsions stabilized with Tween 80 at pH 3.0 and 7.0 exhibited the lowest zeta potential values (Fig. 3), suggesting a more stable oil-in-water emulsion system.⁶¹ Although Tween 80 is a non-ionic surfactant and might be expected to impart a neutral zeta potential, studies have shown that Tween 80-stabilized nanoemulsions often display negative zeta potential values.⁶¹ This negative charge can be

attributed to several factors, including the inherent negative charge of oil droplets due to the presence of anionic hydroxyl groups (OH^-) in the water or oil, and the adsorption of Tween 80 molecules, which can induce negative charges at pH values above 4.0.⁶¹

In comparison to Tween 80, protein-stabilized emulsions exhibited less negative zeta potential values at both pH 3.0 and 7.0. This is likely due to the adsorption of proteins molecules, which shifts the shear plane further from the droplet surface⁹ and introduces positive charges.⁶² At pH 3.0, proteins generally



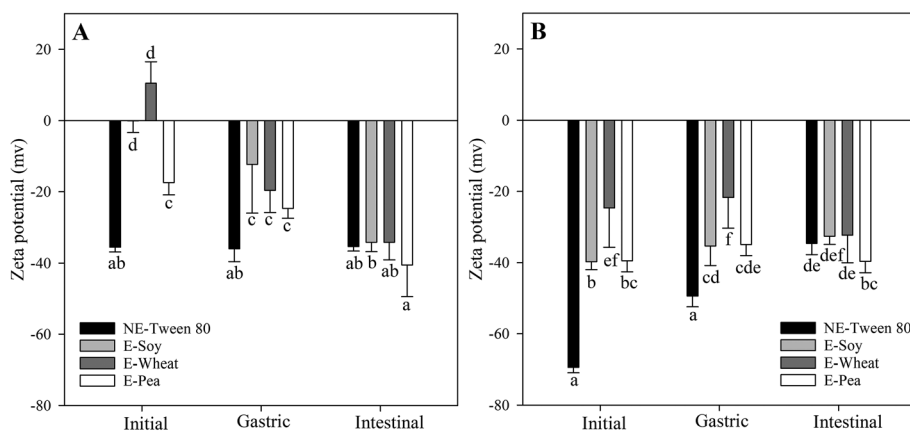


Fig. 3 Zeta potential (mV) of nanoemulsions and emulsions stabilized by Tween 80 (NE-Tween 80), pea (E-Pea), wheat (E-Wheat), and soy (E-Soy) protein isolates during the initial, gastric, and intestinal phases at (A) pH 3.0 or (B) pH 7.0. Different lowercase letters indicate significant differences ($p < 0.05$) within each panel.

carry a positive charge, and their adsorption at the oil-water interface imparts a positive charge to the oil droplets. This effect was particularly pronounced for the emulsion stabilized with wheat protein isolates, consistent with other authors.⁶³ Wheat protein has a higher ratio of basic to acidic amino acids⁶⁴ (a ratio of 15) compared to soy and pea proteins (a ratio of 5) (unpublished data). This can be partly because a large portion of its glutamic acid exists in its amide form, glutamine, which carries a positive charge in acidic environments.^{65,66} Consequently, at an acidic pH of 3.0 (which is well below its isoelectric point, pI), wheat protein develops a strong positive charge. This high charge enhances its natural tendency to adsorb onto the oil-water interface.

Conversely, at pH 7.0, emulsions stabilized with proteins displayed more negative zeta potential values, as proteins tend to become negatively charged at higher pH levels.⁶⁷ Zeta potential data revealed that, at pH 3.0, wheat proteins carried a net positive charge whereas soy and pea remained negatively charged, and at pH 7.0 wheat was still less negatively charged than the other two proteins. This higher net surface charge likely promoted stronger electrostatic attraction and faster diffusion to the negatively charge oil-water interface, helping wheat protein achieve the greatest reduction in IFT, as observed previously (section 3.1 and Fig. 1). This is also in agreement with the findings of Zhou *et al.*²⁴ who reported that wheat protein with less negative zeta potential at alkaline pH exhibited a greater ability to reduce IFT compared to less negative zeta potential at pH 3.0.

The pH dependence of zeta potential in protein-stabilized emulsions can be attributed to changes in the ionization state of carboxyl and amino groups on the protein molecules. At low pH, protonation of these groups ($-\text{NH}_3^+$ and $-\text{COOH}$) leads to prevailing the positive charges. At high pH, deprotonation ($-\text{NH}_2$ and $-\text{COO}^-$) results in a net negative charge.⁶⁸

3.2.3 Dynamic viscosity. Viscosity plays a significant role in food design and can influence lipid digestion, including the release of lipid-soluble bioactive (or health-related) com-

pounds such as β -carotene. Although this study did not specifically investigate viscosity as a modulator of lipid digestion kinetics, the viscosity of the initial emulsions and nanoemulsions was measured to provide deeper insights into their properties and their potential impact on lipid digestion and β -carotene release.

All emulsions and nanoemulsions were prepared using proteins dissolved overnight in buffers adjusted to either pH 3.0 or pH 7.0, as consistently described throughout the study. Fig. 4 presents the viscosity results for emulsions and nanoemulsions stabilized with Tween 80 or plant protein isolates under these specific pH conditions.

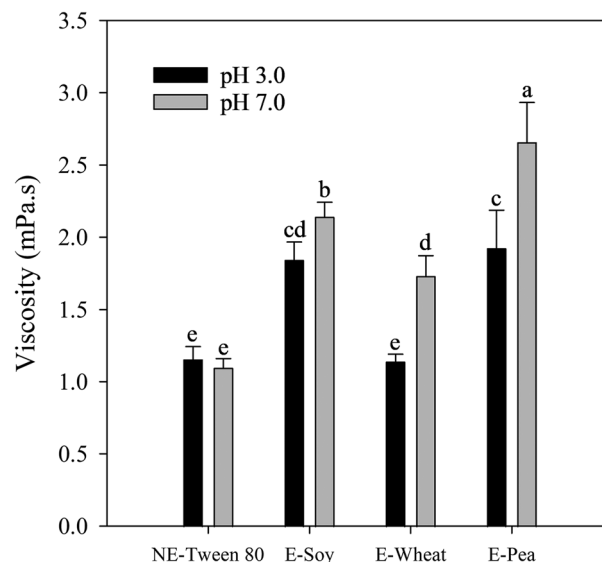


Fig. 4 Viscosity (mPa s) of initial nanoemulsions and emulsions stabilized by Tween 80 (NE-Tween 80), pea (E-Pea), wheat (E-Wheat) or soy (E-Soy) protein isolates at pH 3.0 and pH 7.0. Different letters indicate significant differences among emulsions at different pH ($p < 0.05$).



At pH 3.0, emulsions stabilized with soy and pea proteins showed comparable viscosities (around 1.8–1.9 mPa s), significantly higher than Tween 80-stabilized nanoemulsions (approximately 1.2 mPa s). The smaller droplet size in Tween 80 nanoemulsions allows for easier movement within the dispersion, leading to lower resistance to flow and, consequently, lower viscosity compared to emulsions with larger droplets.⁶⁹ Wheat protein-stabilized emulsions exhibited the lowest viscosity among protein-stabilized samples at this acidic pH (around 1.1 mPa s). These differences correspond well with the observed particle size distribution and microstructure data (section 3.1.2), where smaller droplets in wheat protein emulsions led to reduced flow resistance.

At pH 7.0, viscosity increased for all protein-stabilized emulsions compared to pH 3.0. Specifically, pea protein-stabilized emulsions had the highest viscosity (around 2.7 mPa s), significantly greater than soy protein emulsions (around 2.1 mPa s) and wheat protein emulsions (around 1.7 mPa s). The Tween 80-stabilized nanoemulsion maintained the lowest viscosity (around 1.1 mPa s) at this neutral pH. These findings highlight the significant influence of both protein type and pH conditions on the viscosity of emulsions and nanoemulsions, further impacting their potential behaviour during lipid digestion.

3.2.4 Colloidal stability. The colloidal stability of the emulsions and nanoemulsions was evaluated over the first 24 h after preparation is presented in Fig. 5. These backscattering profiles allow for the detection of early-stage physical instability phenomena that are not yet discernible to the naked eye (SI, Fig. S1). The results showed that Tween 80 (Fig. 5A and B) produced a nanoemulsion with enhanced stability over time. This is consistent with the known emulsion-stabilizing properties of non-ionic surfactants, which primarily rely on a robust steric repulsion mechanism.⁷⁰ The ethylene oxide groups, and long hydrocarbon chain of Tween 80 are thought to contribute to this enhanced steric stabilization.⁷¹ Indeed, Hoeller *et al.*⁷¹ observed that nanoemulsions stabilized with Tween 80 remained physically stable over a 10 week period, with no signs of flocculation, creaming, coalescence, or Ostwald ripening.

In contrast, emulsions stabilized by soy (Fig. 5C and D) and pea (Fig. 5G and H) proteins exhibited notable differences in stability, demonstrating higher stability at pH 7.0 but considerable instability at pH 3.0. This aligns with the particle size and microstructural observations (section 3.1.2). These emulsions displayed substantial creaming at the top and almost complete clarification at the bottom of the tube at both pH levels. Proteins stabilize oil-in-water emulsions by imparting an electrical charge to the droplets, and this process is pH-dependent. Jiang *et al.*⁷² found that soy protein pre-treated at pH 3.5 had a lower emulsifying activity index than at more acidic or alkaline pH values. This reduced activity was attributed to the diminished electrical charge of soy protein near its isoelectric point.

Conversely, wheat protein showed significant stability at pH 3.0 (Fig. 5E) but decreased stability at pH 7.0 (Fig. 5F). These

findings are in agreement with previous studies, which document that wheat gluten exhibits superior solubility and emulsifying properties in acidic conditions (pH 2.0–3.0) compared to near-neutral pH levels (pH 4.0–7.0).⁵³ Emulsion stability is strongly influenced by pH and ionic strength, particularly for protein-stabilized emulsions which are known to flocculate near the isoelectric point of the adsorbed proteins.^{73,74} Since wheat proteins have an isoelectric pH range of 6.0–7.0,⁵⁶ reduced solubility and interfacial activity is expected at pH 7.0, which is close to their isoelectric point. However, at pH 3.0, wheat proteins exhibited noteworthy emulsifying activity, resulting in a highly stable emulsion. At an acidic pH of 3.0, wheat protein undergoes significant conformational and chemical modifications that potentiate its emulsifying properties. The protein acquires a high net positive charge far below its isoelectric point, which induces intramolecular electrostatic repulsion. This force disrupts ordered secondary structures, such as α -helices and β -sheets, promoting partial protein unfolding and increased molecular flexibility.⁷⁵ Concurrently, the acidic conditions facilitate the deamidation of glutamine-rich subunits, particularly the ω -gliadins. This chemical modification, along with subsequent hydrolysis of peptide bonds, results in the generation of lower molecular weight polypeptides. The combined effect of these changes is a molecular population characterized by a less ordered conformation rich in β -turns and composed of smaller, more mobile fragments. These attributes facilitate more rapid diffusion and adsorption at the oil–water interface, enabling the formation of a robust interfacial film that prevents droplet coalescence *via* electrostatic stabilization.⁷⁵ Similarly, Fu *et al.*⁶³ showed that lowering the pH (to about pH 4.0) led to strong electrostatic repulsion between wheat gluten nanoparticles, preventing their aggregation. The enhanced stability of the emulsion emulsified with wheat protein at pH 3.0 can also be attributed to irreversible unfolding of the protein, making it more flexible and surface-active. This is analogous to findings by Jian *et al.*,⁷² who demonstrated that pH-shifting treatment improved the ability of soy proteins to form an interfacial membrane, leading to better oil droplet dispersion compared to native soy proteins. They attributed the heightened surface activity of treated soy protein isolates to increased exposure of hydrophobic amino acid side chains due to partial structural unfolding during treatment. Therefore, the pH likely induced similar structural changes in wheat protein, enhancing its ability to stabilize emulsion droplets.

3.3 Behaviour of o/w emulsions and nanoemulsions during *in vitro* digestion

3.3.1 Particle size and microstructure during *in vitro* digestion. Particle size measurements were conducted following the gastric and intestinal phases of digestion, as shown in Fig. 2. Both emulsions and nanoemulsions exhibited significant increases in droplet size after the gastric phase, indicating widespread coalescence within the chyme. This was further supported by the presence of larger particles in the micrographs (Fig. 2), suggesting ongoing Ostwald ripening under



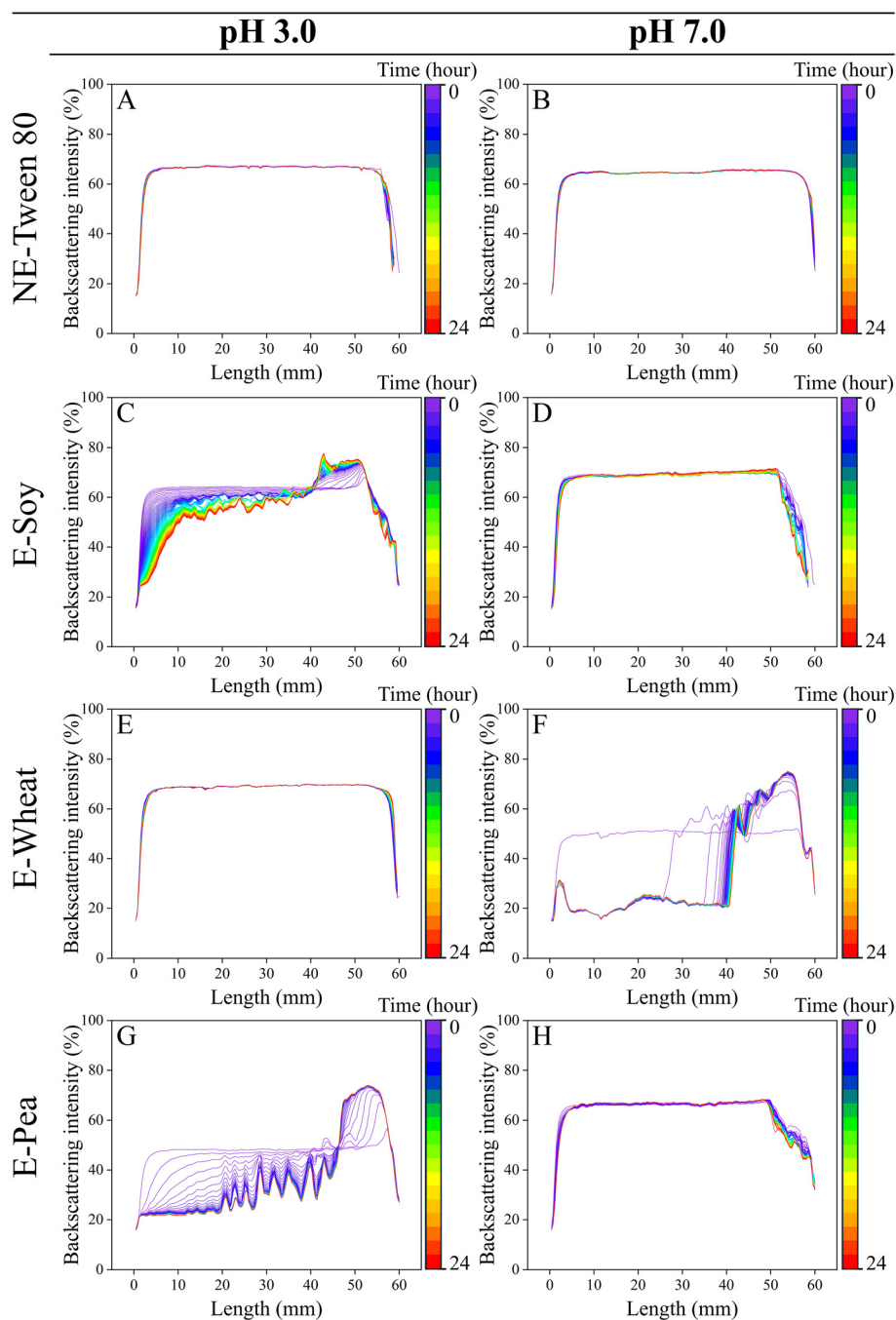


Fig. 5 Turbiscan stability profiles (over the first 24 hours) for nanoemulsions (NE-) and emulsions (E-) stabilized by Tween 80 or plant protein isolates (pea, wheat, soy) at (A, C, E and G) pH 3.0 or (B, D, F and H) pH 7.0.

gastric conditions.⁷⁶ The intestinal phase led to greater polydispersity, with a mixture of small and large clusters consisting of digestion products (FFAs and micelles) and undigested, coalesced oil droplets.

Nanoemulsions stabilized by Tween 80 showed a consistent particle size distribution compared to their respective initial nanoemulsions after the gastric phase at both pH levels. At pH 3.0, a peak at 0.36 μm was observed after the gastric phase and persisted through the intestinal phase. A similar trend was

observed at pH 7.0, with peaks at 0.31 μm and 5.92 μm after both phases. As a non-ionic surfactant, Tween 80 is unaffected by pH changes during the gastric phase, contributing to the high stability of these nanoemulsions under gastric conditions. This colloidal stability is particularly important when studying lipid digestion kinetics during gastrointestinal conditions, as the particle size, and consequently the surface area of lipid dispersions entering the small intestine, can significantly influence digestion dynamics.⁷⁶



Following the gastric phase, all emulsions stabilized with proteins at pH 3.0 displayed multimodal distributions with multiple peaks, indicating the presence of distinct particle populations. Given that the simulated gastric phase was adjusted to pH 3.0, matching the initial pH of the emulsions, the observed differences in their behaviour cannot be attributed primarily to a pH-shift effect. Instead, the presence of pepsin and physical disruption from *in vitro* gastric churning can significantly impact the colloidal structure and stability of protein-stabilized emulsions.⁷⁷ Furthermore, the ionic strength of the simulated gastric fluid and the acidic conditions can induce droplet aggregation by reducing electrostatic repulsion between protein-coated droplets.⁷⁷ Pepsin can also hydrolyse proteins into smaller peptides and amino acids, further weakening the stabilizing protein films and increasing the susceptibility of droplets to coalescence and flocculation. The microscopy images also showed that oil droplets were coalesced and flocculated in the protein-stabilized emulsions during gastric digestion (Fig. 2). Moreover, the stomach's churning action mechanically disrupts emulsion droplets, promoting coalescence and flocculation, thereby exacerbating the destabilizing effects of pH and pepsin.

After the gastric phase, chyme from emulsion stabilized with soy proteins at pH 3.0 exhibited the smallest particle size distribution, with peaks at 0.59 μm , 9.86 μm , and 40.10 μm . Chymes from emulsions stabilized with pea (0.59 μm , 8.68 μm , and 58.90 μm) and wheat proteins (0.59 μm , 7.64 μm , and 45.60 μm) showed remarkably similar distributions, with the chyme from emulsion stabilized with pea protein having the largest particle sizes among the proteins. The smaller particle size of the chyme from emulsion stabilized with soy protein suggests a larger surface area for oil droplets and potentially enhanced susceptibility to pancreatic lipase in the small intestinal phase. Conversely, chyme from emulsion stabilized with pea protein may exhibit comparatively lower digestion rates relative to chyme from emulsion stabilized with wheat protein, highlighting the influence of particle size on digestive processes.

In general, emulsions stabilized with proteins at pH 7.0 exhibited smaller particle size distributions after the gastric phase compared to their counterparts at pH 3.0. The chyme of emulsions stabilized with wheat (0.52 μm , 5.92 μm , and 35.3 μm) and pea proteins (0.59 μm , 7.64 μm , and 35.3 μm) presented larger particle sizes with nearly identical distributions compared to chyme of emulsion stabilized with soy protein (0.59 μm and 3.12 μm). This indicates that emulsions stabilized with wheat and pea proteins at pH 7.0 tend to exhibit larger sizes after the gastric phase, while emulsions stabilized with soy protein maintain a distinctly smaller scale.

After the intestinal phase, for emulsions stabilized with proteins at pH 3.0, the particle size order of the digests was soy protein < wheat protein < pea protein. This order may reflect the extent of digestion, suggesting that the pea protein-stabilized emulsion was less digested compared to those stabilized by wheat and soy proteins. The digest of emulsion stabilized with soy protein exhibited a multimodal distribution with

peaks at 0.52 μm and 11.20 μm , indicating the smallest particle sizes among the proteins. In contrast, digests of emulsions stabilized with wheat (0.52 μm , 12.70 μm , 98.1 μm , and 516 μm) and pea proteins (0.59 μm , 2.13 μm , 12.7 μm , 86.4 μm , and 586 μm) exhibited comparable distributions, with larger particle sizes.

Following the intestinal phase of emulsions stabilized with proteins at pH 7.0, the digest of emulsion stabilized with wheat protein exhibited the largest particle size, with peaks at 0.52 μm , 12.7 μm , and 98.1 μm . The digest of emulsion stabilized with pea protein showed peaks at 0.523 μm , 11.2 μm , and 98.1 μm . Meanwhile, the digest of emulsion stabilized with soy protein had peaks at 0.40 μm , 6.72 μm , and 98.1 μm , representing the smallest particle size distribution among the samples.

These findings suggest that protein-stabilized emulsions undergo more pronounced changes in particle size distribution compared to Tween 80-stabilized nanoemulsions, depending on environmental conditions. Notably, pH plays a critical role in influencing their particle size and morphological properties. After *in vitro* gastric digestion, emulsions stabilized with soy protein exhibited the smaller particle sizes. Furthermore, the presence of residual oil droplets observed in the micrographs of all protein- and Tween 80-stabilized emulsions during the intestinal phase (Fig. 2) suggests that lipid digestion was not fully completed.

3.3.2 Particle charge during *in vitro* digestion. The zeta potential of emulsions and nanoemulsions after *in vitro* gastric and intestinal digestion were measured and presented in Fig. 3. After the gastric phase, chyme of nanoemulsions stabilized with Tween 80, at both pH 3.0 and pH 7.0, exhibited the lowest zeta potential values (-35.95 ± 3.63 mV for pH 3.0 and -49.39 ± 3.02 mV for pH 7.0). This suggests that Tween 80 maintained its integrity at the oil-water interface during gastric digestion, which is consistent with the particle size and micrograph data (section 3.1.2). As previously mentioned, Tween 80's non-ionic nature confers resistance to the changes in ionic strength and pH that occur during the gastric phase.

Protein-stabilized emulsions showed a marked difference in zeta potential depending on whether the proteins were at pH 3.0 or 7.0. This highlights the significant impact of environmental pH on the surface charge and interfacial properties of protein-stabilized emulsions during gastrointestinal digestion. For chyme of emulsions stabilized with proteins at pH 3.0, the zeta potential values were -24.70 ± 2.75 mV (pea), -12.29 ± 13.73 mV (soy), and -19.58 ± 6.24 mV (wheat). These values were less negative than those observed for chyme of emulsions stabilized with proteins at pH 7.0, which were -34.90 ± 3.10 mV (pea), -35.30 ± 5.50 mV (soy), and -21.75 ± 8.54 mV (wheat). Comparing the chyme with the corresponding initial emulsions revealed that emulsions stabilized with proteins at pH 7.0 underwent fewer changes in surface zeta potential during digestion. This is likely because proteins at pH 7.0 have a greater ability to remain adsorbed at the oil-water interface, consistent with the DIFT measurements (Fig. 1).



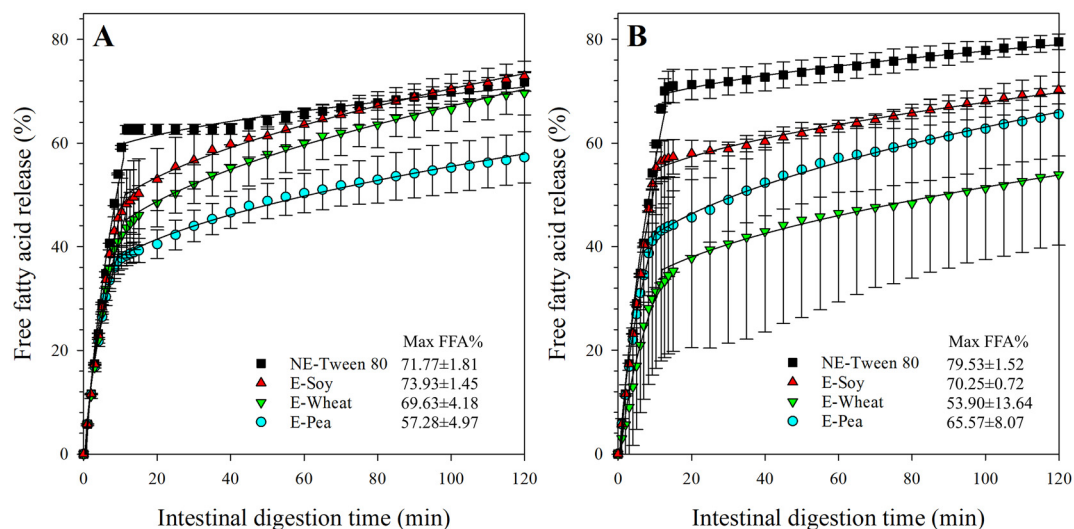


Fig. 6 *In vitro* lipid digestibility expressed as free fatty acid (FFA) release (%) during the intestinal phase (min) of emulsions and nanoemulsions stabilized by Tween 80 ■ or plant protein isolates (pea ●, wheat ▼, soy ▲) at (A) pH 3.0 and (B) pH 7.0. Symbols represent experimental data, solid lines represent model predictions.

3.3.3 *In vitro* lipid digestibility. The release of FFAs during the *in vitro* intestinal phase was monitored to compare the behaviour of different protein emulsifiers (Fig. 6). Nanoemulsion stabilized with Tween 80 showed significantly higher lipolysis ($71.77 \pm 1.81\%$ and $79.53 \pm 1.52\%$, respectively at pH 3.0 and 7.0) than emulsions stabilized with pea and wheat proteins ($p < 0.05$). Although emulsion stabilized with soy protein exhibited lower lipolysis than nanoemulsion stabilized with Tween 80, this difference was not statistically significant ($p > 0.05$). The lipolysis profiles exhibited two distinct phases: an initial rapid phase followed by a slower phase or plateau. To quantify these phases, a power-law model (eqn (3)) was applied, and the resulting parameters, FFA_0 (initial FFA concentration) and k (rate constant), for both phases are summarized in Table 1.

All emulsions displayed biphasic lipolysis, characterized by an initial rapid FFA release phase (k_1) followed by a slower phase or plateau (k_2) (Table 1). This pattern can be attributed to several factors. Initially, high concentrations of bile salts

enhance lipid emulsification and solubilization, increasing the surface area available for lipase activity and leading to rapid triglyceride breakdown. As digestion progresses, the depletion of available triglyceride substrates contributes to a decline in the lipase activity rate. Furthermore, the accumulation of lipolysis products at the oil droplet interface, coupled with a reduced rate of their removal, further slows the release of FFAs. The slow but continuous increase indicates that lipolysis activity was low but still ongoing at the end of the experiments. For emulsions stabilized with proteins at pH 3.0, the slow rate of FFA release during the plateau phase may also be attributed to protein hydrolysis, both at the interface and in the aqueous phase. The resulting hydrolysis products can hinder lipase access to the oil droplet surface, thus slowing down the overall lipid digestion process.

To evaluate the overall effect of the emulsifier, parameter values from both pH levels were pooled for statistical analysis. The analysis revealed that nanoemulsions stabilized with Tween 80 exhibited the highest initial lipolysis rates ($k_1 = 23.13$

Table 1 Estimated kinetic parameters from power law model fitted to free fatty acid (FFA) release data during 120 min of *in vitro* small intestinal digestion. Samples were nanoemulsions and emulsions stabilized by Tween 80 or soy, wheat and pea protein isolates at pH 3.0 or pH 7.0

		FFA ₀ 1 (%)	k_1 (%/min ^{0.5})	R_1^2	t (min)	FFA ₀ 2 (%)	k_2 (% per min ^{0.5})	R_2^2
pH 3.0	NE-Tween 80	-19.30 ± 0.17	23.13 ± 0.10	0.96 ± 0.00	11.09 ± 0.24	55.29 ± 0.26	1.41 ± 0.14	0.92 ± 0.00
	E-Soy	-14.01 ± 1.88	19.63 ± 1.36	0.98 ± 0.00	9.58 ± 0.02	42.51 ± 4.03	2.88 ± 0.28	0.99 ± 0.00
	E-Wheat	-10.46 ± 3.14	16.75 ± 2.71	0.98 ± 0.00	11.34 ± 0.07	33.85 ± 5.55	3.33 ± 0.16	0.99 ± 0.00
	E-Pea	-9.06 ± 1.24	15.63 ± 1.05	0.99 ± 0.00	11.56 ± 0.19	30.06 ± 0.79	2.54 ± 0.39	0.99 ± 0.00
pH 7.0	NE-Tween 80	-21.71 ± 0.97	24.53 ± 0.55	0.96 ± 0.00	12.54 ± 0.54	64.90 ± 3.86	1.28 ± 0.20	0.98 ± 0.00
	E-Soy	-17.00 ± 1.37	21.65 ± 0.90	0.97 ± 0.00	9.98 ± 0.16	48.87 ± 3.29	1.90 ± 0.25	0.98 ± 0.03
	E-Wheat	-10.17 ± 1.30	12.62 ± 4.38	0.94 ± 0.06	12.08 ± 1.58	27.40 ± 23.07	2.40 ± 0.87	0.93 ± 0.08
	E-Pea	-10.87 ± 5.14	16.93 ± 4.06	0.98 ± 0.01	10.14 ± 0.73	32.72 ± 6.67	3.04 ± 0.08	0.99 ± 0.01

FFA₀ is the initial concentration of FFAs, k is the rate constant governing the reaction, and t is the time for FFAs to reach the plateau. The suffixes '1' and '2' denote Phase 1 and Phase 2, respectively.



$\pm 0.10\%/min^{0.5}$ and $24.53 \pm 0.55\%/min^{0.5}$, respectively), and FFA concentration at the transition point (FFA₀₂), followed by emulsions stabilized with soy protein, while emulsions stabilized with pea and wheat proteins showed the lowest values. Although not statistically significant ($p > 0.05$), Tween 80 nanoemulsions consistently showed higher lipolysis than protein-stabilized emulsions. This is likely due to the smaller particle size distribution in Tween 80 nanoemulsions (section 3.1.2), which provides a significantly larger surface area for lipase adsorption and triglyceride breakdown compared to the larger protein-stabilized emulsions.

For emulsions stabilized with proteins at pH 3.0, the initial phase lipolysis rate (k_1) was lower (though not significantly) for pea protein isolates ($15.63 \pm 1.05\%$ per $min^{0.5}$) compared to wheat ($16.75 \pm 2.71\%$ per $min^{0.5}$) and soy protein isolates ($19.63 \pm 1.36\%$ per $min^{0.5}$). Similarly, the second phase lipolysis rate (k_2) was also lower for pea protein isolates ($2.54 \pm 0.39\%$ per $min^{0.5}$) compared to wheat ($3.33 \pm 0.16\%$ per $min^{0.5}$) and (not significantly) to soy protein isolates ($2.88 \pm 0.28\%$ per $min^{0.5}$). Consequently, the pea protein-stabilized emulsion exhibited a slightly, but not significantly, lower overall extent of lipolysis ($57.28 \pm 4.97\%$) compared to those stabilized by wheat ($69.63 \pm 4.18\%$) and soy protein isolates ($73.93 \pm 1.45\%$). The reduced lipolysis with pea protein can be attributed to its lower ability to reduce IFT (Fig. 1) and its lower stability (Fig. 5G) at pH 3.0. This inadequate oil droplet coverage likely led to protein aggregation and oil droplet coalescence during the gastric phase, resulting in the largest observed particle size in the chyme for this emulsion (Fig. 2). The reduced oil droplet surface area upon entering the intestinal phase consequently contributed to the lower lipolysis rate observed for the pea protein emulsion. The slightly higher digestibility of the soy and wheat protein emulsions compared to the pea protein emulsion can be attributed to two potential factors. First, after simulated gastric digestion at pH 3.0, the soy and wheat emulsions had smaller particle sizes (Fig. 2), which provides a larger surface area for proteolytic enzymes. Second, protein secondary structure influences enzymatic accessibility, as a high content of rigid β -sheet structures typically reduces digestibility. This is relevant because wheat gluten contains a lower proportion of β -sheets than pea protein, likely contributing to the higher digestibility observed in the wheat protein emulsion.⁷⁸

For emulsions stabilized with proteins at pH 7.0 (Fig. 6B), the emulsion stabilized with wheat protein isolates showed the lowest extent of lipolysis ($53.90 \pm 13.64\%$), although this was not significantly different from emulsions stabilized with soy ($70.25 \pm 0.72\%$) or pea protein isolates ($65.57 \pm 8.07\%$). This can be attributed to the instability of the wheat protein emulsion at pH 7.0, which resulted in particle aggregation and coalescence, reducing the available surface area for lipase action and hindering lipase diffusion.

While the findings of this study provide valuable mechanistic insights, it is important to acknowledge the inherent limitations of the static *in vitro* digestion model utilized. Static models cannot fully replicate the complex physiochemical and

physiological processes occurring within the human gastrointestinal tract. Specifically, the simplified physiological conditions such as constant pH steps and fixed enzyme ratios lack the dynamic peristalsis, gradual gastric emptying, and continuous fluid secretions present *in vivo*.⁷⁹ Furthermore, this model assesses bioaccessibility rather than true bioavailability, as it does not account for the complex processes of epithelial transport and cellular uptake across the intestinal mucosa, nor does it simulate the metabolic transformations mediated by the gut microbiota in the lower gastrointestinal tract.⁸⁰ Despite these constraints, static *in vitro* models are highly recognized for their utility in rapidly screening the influence of food matrix composition and identifying the interfacial properties of delivery systems that govern their digestive fate. Importantly, numerous studies have demonstrated that *in vitro* digestion models similar to the one employed in this work yield bioaccessibility trends that positively correlate with *in vivo* outcomes.⁵

3.3.4 β -carotene bioaccessibility. In this study, β -carotene bioaccessibility was relatively low, ranging from 9.04 to 13.41% depending on the emulsifier and pH (Fig. 7). The pH (3.0 vs. 7.0) did not significantly change β -carotene bioaccessibility ($p > 0.05$). Numerically, emulsions stabilized by wheat protein showed the highest mean bioaccessibility at both pH values ($12.61 \pm 1.03\%$ at pH 3.0, and $13.41 \pm 4.09\%$ at pH 7.0), and were slightly but not significantly ($p > 0.05$) higher than the Tween 80 nanoemulsion (around 11%). In contrast, emulsions stabilized by soy and pea proteins were lower (around 9 to 10%).

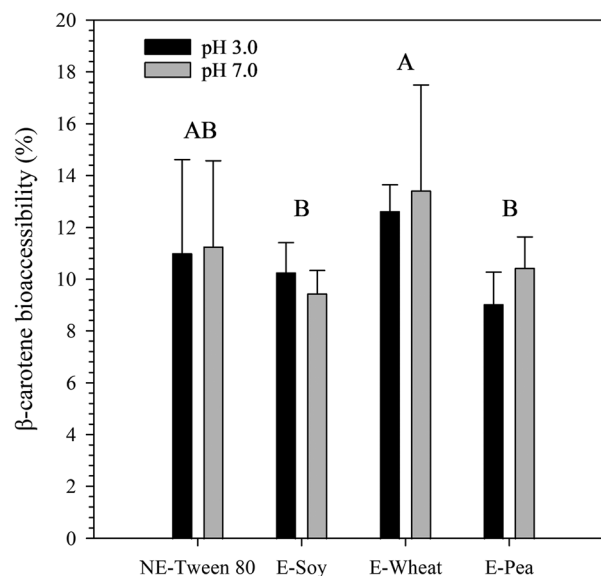


Fig. 7 β -Carotene bioaccessibility (%) in the micellar phase after 120 min of *in vitro* intestinal digestion of emulsions and nanoemulsions stabilized by Tween 80 or plant protein isolates (soy, wheat, pea) at pH 3.0 or pH 7.0. Different letters indicate overall significant differences of β -carotene bioaccessibility values among emulsions regarding their emulsifier type ($p < 0.05$).



These values are in line with those observed in several emulsion systems stabilized by plant proteins. For example, Fu *et al.*⁶³ reported that emulsions stabilized by wheat gluten nanoparticles had bioaccessibility values starting around 11%, which improved when combined with other stabilizers. Similarly, pea protein-stabilized systems have been reported to exhibit β -carotene bioaccessibility around 8.53%,¹¹ while soy protein isolate-stabilized emulsions showed values around 10.6%.⁸¹ Collectively, these studies support the view that plant-protein interfaces can yield modest carotenoid bioaccessibility, often constrained by digestion-driven interactions among proteins, bile salts, and lipid digestion products.

Multiple mechanisms have been proposed to explain low β -carotene bioaccessibility in protein-stabilized systems. One widely discussed limitation is the interaction between plant proteins (or their digestion products) and bile salts, which can promote the formation of insoluble aggregates during digestion. Such aggregates may physically entrap β -carotene and reduce its transfer into mixed micelles.⁶³ In addition, gastric proteolysis can weaken the interfacial layer. When interfacial proteins are degraded, droplets may become more prone to coalescence, increasing the mean droplet size and decreasing the accessible interfacial area for lipase action. This can reduce free fatty acid release, limiting mixed micelle formation and ultimately restricting the solubilization of β -carotene into the micellar phase.⁸¹ Other factors reported to further depress bioaccessibility include (i) incomplete intestinal lipid digestion associated with relatively large droplet size, and (ii) chemical degradation of β -carotene under harsh gastric conditions, including isomerization and/or oxidation in highly acidic environments.¹¹

When positioned within the broader literature, our results fall between two extremes that have been reported for emulsion-based delivery systems. On one hand, much lower bioaccessibility values (about 1 to 3%) have been reported.⁸² In that study, changing the emulsifier from protein to Tween 20 increased β -carotene bioaccessibility dramatically (from 1 to 3% up to 72.5%), highlighting how strongly interfacial composition can control micellarization.⁸² Furthermore, the low values in protein-stabilized systems were attributed either to direct carotenoid–protein interactions or to electrostatic interactions between anionic mixed micelles and cationic protein molecules that could hinder micelle formation and carotenoid incorporation.⁸² Lipid composition is also critical, since emulsions formulated with short-chain fatty acids have been reported to show much lower (about 1%) bioaccessibility than those containing long-chain fatty acids (about 41%).⁸³ These observations are consistent with the concept that both interfacial interactions and the nature of digestion products (long-chain fatty acids and their ability to form mixed micelles) can strongly modulate carotenoid bioaccessibility.

On the other hand, considerably higher bioaccessibility values have been reported, ranging from 26.98% up to 70.1%.^{84,85} Across these studies, higher bioaccessibility has been linked to several converging factors: higher oil content and thus greater release of free fatty acids during digestion,⁸⁴

the use of multilayer or tertiary emulsions that can increase bioaccessibility more than two-fold (from around 30% to around 70%),⁸⁵ and digestive conditions that provide a higher lipase-to-lipid and bile-to-lipid ratio, thereby ensuring sufficient mixed micelles to incorporate released β -carotene.⁸³ In addition, chemical or physical protection of bioactive during digestion, for example *via* antioxidants or interfacial architectures that reduce degradation, has been described as beneficial.^{11,84,85} Conversely, systems that avoid emulsifier-bioactive interactions that interfere with micellar incorporation have been associated with higher bioaccessibility.⁸⁶ Finally, combining proteins with other surface-active components has repeatedly been highlighted as an effective strategy to enhance bioaccessibility,¹¹ consistent with reports where wheat gluten nanoparticle systems improved upon inclusion of complementary stabilizers.⁶³

Within our own dataset, the higher bioaccessibility observed for wheat protein emulsions compared with pea and soy emulsions suggests that wheat proteins may have promoted more effective micelle formation. One possible explanation is a stronger contribution from wheat protein hydrolysates generated during gastric digestion. Since proteins adsorbed at the oil–water interface are more prone to proteolysis,⁸⁷ and considering the lower IFT of wheat protein (Fig. 1), wheat proteins may have been more effectively positioned at the interface, leading to more extensive proteolysis during the gastric phase. The resulting hydrolysates could then facilitate mixed micelle formation and/or reduce interfacial constraints on lipolysis, ultimately enhancing β -carotene transfer into the micellar phase. Overall, the literature consistently shows that β -carotene bioaccessibility is highly sensitive to interfacial composition and digestive conditions, which helps explain why reported values can span from about 1% to more than 70%.^{85,88,89}

4. Conclusions

This study demonstrates that plant proteins offer a viable alternative to synthetic surfactants like Tween 80, provided that the formulation pH is selected in relation to each protein's isoelectric region and aggregation tendency. While the benchmark Tween 80 remained stable across all conditions, wheat protein at pH 3.0 formed highly stable emulsions that facilitated efficient lipolysis and β -carotene bioaccessibility comparable to the synthetic surfactant, highlighting its potential for acidic food matrices. In contrast, soy and pea proteins required neutral conditions to minimize aggregation, supporting their use as clean-label emulsifiers for near-neutral formulations. These results emphasize that the choice of plant protein emulsifier should be guided by the intended product matrix, particularly its pH, and having established these fundamental mechanisms in a controlled *in vitro* setting, these results can serve as a basis for future research to validate their performance within more complex, dynamic biological environments.



Author contributions

Mohsen Ramezani: conceptualization, methodology, data curation, formal analysis, investigation, software, visualization, validation, writing original draft, writing – review and editing. Marga Amengual Ramon: investigation. Laura Salvia-Trujillo: conceptualization, methodology, funding acquisition, project administration, supervision, resources, writing – review and editing. Olga Martín-Belloso: conceptualization, methodology, funding acquisition, supervision, resources, writing – review and editing, project administration.

Conflicts of interest

There are no conflicts to declare.

Data availability

Data for this article, including the spreadsheets detailing colloidal stability (interfacial tension, particle size, zeta potential, viscosity, backscattering intensity), pH-stat monitoring of lipolysis, and Beta-carotene bioaccessibility analysis throughout the initial, gastric and intestinal phases are available at CORA. Repositori de Dades de Recerca at <https://doi.org/10.34810/data2788>.⁹⁰

The data supporting this article including the visual appearance of nanoemulsions (NE-) and emulsions (E-) after 24 hours stabilized by Tween 80 or plant protein isolates (pea, wheat, soy) at pH 3.0 or pH 7.0. have been included as part of the supplementary information (SI). See DOI: <https://doi.org/10.1039/d5fo05533d>.

Acknowledgements

This study was funded by the Ministry of Economy, Industry and Competitiveness (MINECO/FEDER, UE) throughout project PID2022-137838OB-I00. Moreover, this project has received funding from the MCIU, AEI, FEDER, UE [grant number RTI2018-094268-B-C21], and the European Union's H2020 research and innovation programme under Marie Skłodowska-Curie [grant agreement No 801586]. The authors thank Agrotecnio and IRBLleida for the funding of through the Call for Joint Research Projects on Agriculture, Food, Nutrition and Health – AgroHealth2024, with the project AGRHLTH24-1.

References

- N. I. Krinsky and E. J. Johnson, Carotenoid Actions and Their Relation to Health and Disease, *Mol. Aspects Med.*, 2005, **26**(6), 459–516, DOI: [10.1016/j.mam.2005.10.001](https://doi.org/10.1016/j.mam.2005.10.001).
- C. S. Boon, D. J. McClements, J. Weiss and E. A. Decker, Factors Influencing the Chemical Stability of Carotenoids in Foods, *J. Crit Rev Food Sci. Nutr.*, 2010, **50**(6), 515–532, DOI: [10.1080/10408390802565889](https://doi.org/10.1080/10408390802565889).
- D. A. Garrett, M. L. Failla and R. J. Sarama, Development of an in Vitro Digestion Method to Assess Carotenoid Bioavailability from Meals, *J. Agric. Food Chem.*, 1999, **47**(10), 4301–4309, DOI: [10.1021/jf9903298](https://doi.org/10.1021/jf9903298).
- C. P. Tan and M. Nakajima, β -Carotene Nanodispersions: Preparation, Characterization and Stability Evaluation, *Food Chem.*, 2005, **92**(4), 661–671, DOI: [10.1016/j.foodchem.2004.08.044](https://doi.org/10.1016/j.foodchem.2004.08.044).
- L. Salvia-Trujillo, C. Qian, O. Martín-Belloso and D. J. McClements, Influence of Particle Size on Lipid Digestion and β -Carotene Bioaccessibility in Emulsions and Nanoemulsions, *Food Chem.*, 2013, **141**(2), 1472–1480, DOI: [10.1016/j.foodchem.2013.03.050](https://doi.org/10.1016/j.foodchem.2013.03.050).
- Z. Wang, M. A. Neves, H. Isoda and M. Nakajima, Preparation and Characterization of Micro/Nano-Emulsions Containing Functional Food Components, *Japan J. Food Eng.*, 2015, **16**(4), 263–276, DOI: [10.11301/jfsfe.16.263](https://doi.org/10.11301/jfsfe.16.263).
- D. J. McClements and C. E. Gumus, Natural Emulsifiers—Biosurfactants, Phospholipids, Biopolymers, and Colloidal Particles: Molecular and Physicochemical Basis of Functional Performance, *Adv. Colloid Interface Sci.*, 2016, **234**, 3–26, DOI: [10.1016/j.cis.2016.03.002](https://doi.org/10.1016/j.cis.2016.03.002).
- D. Webb, H. Dogan, Y. Li and S. Alavi, Physico-Chemical Properties and Texturization of Pea, Wheat and Soy Proteins Using Extrusion and Their Application in Plant-Based Meat, *Foods*, 2023, **12**(8), 1586, DOI: [10.3390/foods12081586](https://doi.org/10.3390/foods12081586).
- Y. Jiao, Y. Zhao, Y. Chang, Z. Ma, I. Kobayashi, M. Nakajima and M. A. Neves, Enhancing the Formation and Stability of Oil-In-Water Emulsions Prepared by Microchannels Using Mixed Protein Emulsifiers, *Front. Nutr.*, 2022, **9**, 822053, DOI: [10.3389/fnut.2022.822053](https://doi.org/10.3389/fnut.2022.822053).
- S. Li, Y. Zhu, X. Hao, H. Su, X. Chen and Y. Yao, High Internal Phase Pickering Emulsions Stabilized by the Complexes of Ultrasound-Treated Pea Protein Isolate/Mung Bean Starch for Delivery of β -Carotene, *Food Chem.*, 2024, **440**, 138201, DOI: [10.1016/j.foodchem.2023.138201](https://doi.org/10.1016/j.foodchem.2023.138201).
- Q. Guo, I. Bayram, X. Shu, J. Su, W. Liao, Y. Wang and Y. Gao, Improvement of Stability and Bioaccessibility of β -Carotene by Curcumin in Pea Protein Isolate-Based Complexes-Stabilized Emulsions: Effect of Protein Complexation by Pectin and Small Molecular Surfactants, *Food Chem.*, 2022, **367**, 130726, DOI: [10.1016/j.foodchem.2021.130726](https://doi.org/10.1016/j.foodchem.2021.130726).
- Y. Wei, D. Zhou, A. Mackie, S. Yang, L. Dai, L. Zhang, L. Mao and Y. Gao, Stability, Interfacial Structure, and Gastrointestinal Digestion of β -Carotene-Loaded Pickering Emulsions Co-Stabilized by Particles, a Biopolymer, and a Surfactant, *J. Agric. Food Chem.*, 2021, **69**(5), 1619–1636, DOI: [10.1021/acs.jafc.0c06409](https://doi.org/10.1021/acs.jafc.0c06409).
- F. Luo, M. Jian, L. Li, J. Xiao, S. Li, N. Zhang and Z. Zhu, Stability and Bioavailability of β -Carotene-Loaded Emulsions Improved by Covalent Interactions between Soybean Protein Isolate, Myricetin, and β -Glucan,



- Int. J. Biol. Macromol.*, 2025, **332**, 147912, DOI: [10.1016/j.ijbiomac.2025.147912](https://doi.org/10.1016/j.ijbiomac.2025.147912).
- 14 C. Dai, S. Han, C. Ma, D. J. McClements, D. Xu, S. Chen, X. Liu and F. Liu, High Internal Phase Emulsions Stabilized by Pea Protein Isolate-EGCG-Fe³⁺ Complexes: Encapsulation of β -Carotene, *Food Hydrocolloids*, 2024, **150**, 109607, DOI: [10.1016/j.foodhyd.2023.109607](https://doi.org/10.1016/j.foodhyd.2023.109607).
 - 15 P. J. Davis and S. C. Williams, Protein Modification by Thermal Processing, *Allergy*, 1998, **53**(SUPPL. 46), 102–105, DOI: [10.1111/j.1398-9995.1998.tb04975.x](https://doi.org/10.1111/j.1398-9995.1998.tb04975.x).
 - 16 H. M. Zbikowska, P. Nowak and B. Wachowicz, Protein Modification Caused by a High Dose of Gamma Irradiation in Cryo-Sterilized Plasma: Protective Effects of Ascorbate, *Free Radicals Biol. Med.*, 2006, **40**(3), 536–542, DOI: [10.1016/j.freeradbiomed.2005.09.012](https://doi.org/10.1016/j.freeradbiomed.2005.09.012).
 - 17 J. Zhang, S. Zhao, L. Li, B. Kong and H. Liu, High Internal Phase Emulsions Stabilized by Pea Protein Isolate Modified by Ultrasound Combined with PH-Shifting: Micromorphology, Rheology, and Physical Stability, *Foods*, 2023, **12**(7), 1433, DOI: [10.3390/foods12071433](https://doi.org/10.3390/foods12071433).
 - 18 S. J. Ge and L. X. Zhang, Control of the Degree of Hydrolysis of a Protein Modification with Immobilized Protease by the PH-Drop Method, *Eng. Life Sci.*, 1993, **13**(2), 151–160, DOI: [10.1002/abio.370130214](https://doi.org/10.1002/abio.370130214).
 - 19 J. Zhao, S. Wang, D. Jiang, C. Chen, J. Tang, I. Tomasevic and W. Sun, The Influence of Protein Oxidation on Structure, Pepsin Diffusion, and in Vitro Gastric Digestion of SPI Emulsion, *Food Chem.*, 2023, **428**, 136791, DOI: [10.1016/j.foodchem.2023.136791](https://doi.org/10.1016/j.foodchem.2023.136791).
 - 20 Y. R. Tang, A. K. Stone, Y. Wang, L. Zhou, J. Kimmel, J. D. House and M. T. Nickerson, Effect of a PH Shift Treatment on the Functional Properties of Individual and Blended Commercial Plant Protein Ingredients, *Eur. Food Res. Technol.*, 2023, **249**(8), 1969–1977, DOI: [10.1007/s00217-023-04267-0](https://doi.org/10.1007/s00217-023-04267-0).
 - 21 J. Jiang, Q. Wang and Y. L. Xiong, A PH Shift Approach to the Improvement of Interfacial Properties of Plant Seed Proteins, *Curr. Opin. Food Sci.*, 2018, **19**, 50–56, DOI: [10.1016/j.cofs.2018.01.002](https://doi.org/10.1016/j.cofs.2018.01.002).
 - 22 A. C. Dumetz, A. M. Chockla, E. W. Kaler and A. M. Lenhoff, Effects of PH on Protein-Protein Interactions and Implications for Protein Phase Behavior, *Biochim. Biophys. Acta, Proteins Proteomics*, 2008, **1784**(4), 600–610, DOI: [10.1016/j.bbapap.2007.12.016](https://doi.org/10.1016/j.bbapap.2007.12.016).
 - 23 N. V. Di Russo, D. A. Estrin, M. A. Martí and A. E. Roitberg, PH-Dependent Conformational Changes in Proteins and Their Effect on Experimental PKas: The Case of Nitrophorin 4, *PLoS Comput. Biol.*, 2012, **8**(11), e1002761, DOI: [10.1371/journal.pcbi.1002761](https://doi.org/10.1371/journal.pcbi.1002761).
 - 24 B. Zhou, X. Cao, Y. Rong, C. Wu, Y. Hu, B. Li and B. Cui, Emulsifying and Interfacial Properties of Glutenin Processed by PH-Shifting Treatment, *J. Mol. Liq.*, 2024, **403**, 124889, DOI: [10.1016/j.molliq.2024.124889](https://doi.org/10.1016/j.molliq.2024.124889).
 - 25 Y. Wang and B. Vardhanabhuti, The Influence of PH on the Emulsification Properties of Heated Whey Protein-Pectin Complexes, *Foods*, 2024, **13**(14), 2295, DOI: [10.3390/foods13142295](https://doi.org/10.3390/foods13142295).
 - 26 H. Lee, G. Yildiz, L. C. dos Santos, S. Jiang, J. E. Andrade, N. J. Engeseth and H. Feng, Soy Protein Nano-Aggregates with Improved Functional Properties Prepared by Sequential PH Treatment and Ultrasonication, *Food Hydrocolloids*, 2016, **55**, 200–209, DOI: [10.1016/j.foodhyd.2015.11.022](https://doi.org/10.1016/j.foodhyd.2015.11.022).
 - 27 M. Iddir, F. Vahid, D. Merten, Y. Larondelle and T. Bohn, Influence of Proteins on the Absorption of Lipophilic Vitamins, Carotenoids and Curcumin, A Review, *Mol. Nutr. Food Res.*, 2022, **66**(13), e2200076, DOI: [10.1002/mnfr.202200076](https://doi.org/10.1002/mnfr.202200076).
 - 28 H. Dai, F. Zhan, Y. Chen, Q. Shen, F. Geng, Z. Zhang and B. Li, Improvement of the Solubility and Emulsification of Rice Protein Isolate by the PH Shift Treatment, *Int. J. Food Sci. Technol.*, 2023, **58**(1), 355–366, DOI: [10.1111/ijfs.15834](https://doi.org/10.1111/ijfs.15834).
 - 29 G. R. Velderrain-Rodríguez, L. Salvia-Trujillo, G. A. González-Aguilar and O. Martín-Belloso, Interfacial Activity of Phenolic-Rich Extracts from Avocado Fruit Waste: Influence on the Colloidal and Oxidative Stability of Emulsions and Nanoemulsions, *Innovative Food Sci. Emerging Technol.*, 2021, **69**, 102665, DOI: [10.1016/j.ifset.2021.102665](https://doi.org/10.1016/j.ifset.2021.102665).
 - 30 F. K. Mwiiri and R. Daniels, Optimized Birch Bark Extract-Loaded Colloidal Dispersion Using Hydrogenated Phospholipids as Stabilizer, *Pharmaceutics*, 2020, **12**(9), 832, DOI: [10.3390/pharmaceutics12090832](https://doi.org/10.3390/pharmaceutics12090832).
 - 31 P. Borel, P. Grolier, M. Armand, A. Partier, H. Lafont, D. Lairon and V. Azais-Braesco, Carotenoids in Biological Emulsions: Solubility, Surface-to-Core Distribution, and Release from Lipid Droplets, *J. Lipid Res.*, 1996, **37**(2), 250–261, DOI: [10.1016/S0022-2275\(20\)37613-6](https://doi.org/10.1016/S0022-2275(20)37613-6).
 - 32 M. Ramezani, L. Salvia-Trujillo and O. Martín-Belloso, Modulating Edible-Oleogels Physical and Functional Characteristics by Controlling Their Microstructure, *Food Funct.*, 2024, **15**(2), 663–675, DOI: [10.1039/D3FO03491G](https://doi.org/10.1039/D3FO03491G).
 - 33 P. K. Okuro, M. Viau, S. Marze, S. Laurent, R. L. Cunha, C. Berton-Carabin and A. Meynier, In Vitro Digestion of High-Lipid Emulsions: Towards a Critical Interpretation of Lipolysis, *Food Funct.*, 2023, **14**(24), 10868–10881, DOI: [10.1039/d3fo03816e](https://doi.org/10.1039/d3fo03816e).
 - 34 J. Calvo-Lerma, V. Fornés-Ferrer, A. Heredia and A. Andrés, In Vitro Digestion Models to Assess Lipolysis: The Impact of the Simulated Conditions on Gastric and Intestinal PH, Bile Salts and Digestive Fluids, *Food Res. Int.*, 2019, **125**, 108511, DOI: [10.1016/j.foodres.2019.108511](https://doi.org/10.1016/j.foodres.2019.108511).
 - 35 M. Ramezani, O. Martín-Belloso and L. Salvia-Trujillo, Influence of Oleogel Composition on Lipid Digestibility and β -Carotene Bioaccessibility during in Vitro Digestion, *Food Chem.*, 2024, **456**, 139978, DOI: [10.1016/j.foodchem.2024.139978](https://doi.org/10.1016/j.foodchem.2024.139978).
 - 36 A. Pérez-Gálvez, In Vitro Digestion Protocols. The Benchmark for Estimation of In Vivo Data. in *Carotenoid Esters in Foods: Physical, Chemical and Biological Properties*,



- ed. A. Z. Mercadante, Royal Society of Food Chemistry, 2019, pp. 421–458. DOI: [10.1039/9781788015851-00421](https://doi.org/10.1039/9781788015851-00421).
- 37 G. Velderrain-Rodríguez, C. Fontes-Candia, A. López-Rubio, M. Martínez-Sanz, O. Martín-Belloso and L. Salvia-Trujillo, Polysaccharide-Based Structured Lipid Carriers for the Delivery of Curcumin: An in Vitro Digestion Study, *Colloids Surf., B*, 2023, **227**, 113349, DOI: [10.1016/j.colsurfb.2023.113349](https://doi.org/10.1016/j.colsurfb.2023.113349).
- 38 C. Fontes-Candia, J. C. Martínez, A. López-Rubio, L. Salvia-Trujillo, O. Martín-Belloso and M. Martínez-Sanz, Emulsion Gels and Oil-Filled Aerogels as Curcumin Carriers: Nanostructural Characterization of Gastrointestinal Digestion Products, *J. Food Chem.*, 2022, **387**, 132877, DOI: [10.1016/j.foodchem.2022.132877](https://doi.org/10.1016/j.foodchem.2022.132877).
- 39 Y. Tan, Z. Zhang, H. Zhou, H. Xiao and D. J. McClements, Factors Impacting Lipid Digestion and SS-Carotene Bioaccessibility Assessed by Standardized Gastrointestinal Model (INFOGEST): Oil Droplet Concentration, *Food Funct.*, 2020, **11**(8), 7126–7137, DOI: [10.1039/d0fo01506g](https://doi.org/10.1039/d0fo01506g).
- 40 F. D. Gunstone, *Fatty Acid and Lipid Chemistry*, Springer US: Fife, UK, First edit., 1996. DOI: [10.1007/978-1-4615-4131-8](https://doi.org/10.1007/978-1-4615-4131-8).
- 41 L. M. Canfield, T. A. Fritz and T. E. Tarara, Incorporation of β -Carotene into Mixed Micelles, *Methods Enzymol.*, 1990, **189**, 418–422, DOI: [10.1016/0076-6879\(90\)89316-a](https://doi.org/10.1016/0076-6879(90)89316-a).
- 42 L. Salvia-Trujillo, S. Verkempinck, S. K. Rijal, A. Van Loey, T. Grauwet and M. Hendrickx, Lipid Nanoparticles with Fats or Oils Containing β -Carotene: Storage Stability and in Vitro Digestibility Kinetics, *Food Chem.*, 2019, **278**, 396–405, DOI: [10.1016/j.foodchem.2018.11.039](https://doi.org/10.1016/j.foodchem.2018.11.039).
- 43 M. H. Wu, H. H. Yan, Z. Q. Chen and M. He, Effects of Emulsifier Type and Environmental Stress on the Stability of Curcumin Emulsion, *J. Dispersion Sci. Technol.*, 2017, **38**(10), 1375–1380, DOI: [10.1080/01932691.2016.1227713](https://doi.org/10.1080/01932691.2016.1227713).
- 44 J. O'Sullivan, B. Murray, C. Flynn and I. Norton, Comparison of Batch and Continuous Ultrasonic Emulsification Processes., *J. Food Eng.*, 2015, **167**, 114–121, DOI: [10.1016/j.jfoodeng.2015.05.001](https://doi.org/10.1016/j.jfoodeng.2015.05.001).
- 45 C.-Y. Chang, J.-D. Jin, H.-L. Chang, K.-C. Huang, Y.-F. Chiang, M. Ali and S.-M. Hsia, Antioxidative Activity of Soy, Wheat and Pea Protein Isolates Characterized by Multi-Enzyme Hydrolysis, *Nanomaterials*, 2021, **11**(6), 1509, DOI: [10.3390/nano11061509](https://doi.org/10.3390/nano11061509).
- 46 J. Gould and B. Wolf, Interfacial and Emulsifying Properties of Mealworm Protein at the Oil/Water Interface, *Food Hydrocolloids*, 2018, **77**, 57–65, DOI: [10.1016/j.foodhyd.2017.09.018](https://doi.org/10.1016/j.foodhyd.2017.09.018).
- 47 M. A. Bos and T. Van Vliet, Interfacial, Rheological Properties of Adsorbed Protein Layers and Surfactants: A Review, *Adv. Colloid Interface Sci.*, 2001, **91**(3), 437–471, DOI: [10.1016/S0001-8686\(00\)00077-4](https://doi.org/10.1016/S0001-8686(00)00077-4).
- 48 A. C. Y. Lam, A. Can Karaca, R. T. Tyler and M. T. Nickerson, Pea Protein Isolates: Structure, Extraction, and Functionality, *Food Rev. Int.*, 2018, **34**(2), 126–147, DOI: [10.1080/87559129.2016.1242135](https://doi.org/10.1080/87559129.2016.1242135).
- 49 M. Shimizu, M. Saito and K. Yamauchi, Emulsifying and Structural Properties of β -Lactoglobulin at Different PHs, *Agric. Biol. Chem.*, 1985, **49**(1), 189–194, DOI: [10.1080/00021369.1985.10866680](https://doi.org/10.1080/00021369.1985.10866680).
- 50 R. E. Aluko, O. A. Mofolasayo and B. M. Watts, Emulsifying and Foaming Properties of Commercial Yellow Pea (*Pisum Sativum* L.) Seed Flours, *J. Agric. Food Chem.*, 2009, **57**(20), 9793–9800, DOI: [10.1021/jf902199x](https://doi.org/10.1021/jf902199x).
- 51 A. Gharsallaoui, E. Cases, O. Chambin and R. Saurel, Interfacial and Emulsifying Characteristics of Acid-Treated Pea Protein, *Food Biophys.*, 2009, **4**(4), 273–280, DOI: [10.1007/s11483-009-9125-8](https://doi.org/10.1007/s11483-009-9125-8).
- 52 L. Salvia-Trujillo, E. A. Decker and D. J. McClements, Influence of an Anionic Polysaccharide on the Physical and Oxidative Stability of Omega-3 Nanoemulsions: Antioxidant Effects of Alginate, *Food Hydrocolloids*, 2016, **52**, 690–698, DOI: [10.1016/j.foodhyd.2015.07.035](https://doi.org/10.1016/j.foodhyd.2015.07.035).
- 53 U. S. van der Schaaf, J. Schreck, V. L. Pietsch and H. P. Karbstein, Wheat Gluten Stabilized Emulsions: Influence of Homogenization Process, PH, and Ethanol Concentration on Droplet Breakup and Stabilization., *J. Food Eng.*, 2020, **287**, 110136, DOI: [10.1016/j.jfoodeng.2020.110136](https://doi.org/10.1016/j.jfoodeng.2020.110136).
- 54 H. N. Liang and C. H. Tang, PH-Dependent, Emulsifying Properties of Pea [*Pisum Sativum* (L.)] Proteins, *Food Hydrocolloids*, 2013, **33**(2), 309–319, DOI: [10.1016/j.foodhyd.2013.04.005](https://doi.org/10.1016/j.foodhyd.2013.04.005).
- 55 J. M. Franco, P. Partal, D. Ruiz-M rquez, B. Conde and C. Gallegos, Influence of PH and Protein Thermal Treatment on the Rheology of Pea Protein-Stabilized Oil-in-Water Emulsions, *J. Am. Oil Chem. Soc.*, 2000, **77**(9), 975–984, DOI: [10.1007/s11746-000-0154-x](https://doi.org/10.1007/s11746-000-0154-x).
- 56 H. Zhao, C. Shen, Z. Wu, Z. Zhang and C. Xu, Comparison of Wheat, Soybean, Rice, and Pea Protein Properties for Effective Applications in Food Products, *J. Food Biochem.*, 2020, **44**(4), e13157, DOI: [10.1111/jfbc.13157](https://doi.org/10.1111/jfbc.13157).
- 57 Z. Zuo, X. Zhang, T. Li, J. Zhou, Y. Yang, X. Bian and L. Wang, High Internal Phase Emulsions Stabilized Solely by Sonicated Quinoa Protein Isolate at Various PH Values and Concentrations, *Food Chem.*, 2022, **378**, 132011, DOI: [10.1016/j.foodchem.2021.132011](https://doi.org/10.1016/j.foodchem.2021.132011).
- 58 J. S. J. Santiago, L. Salvia-Trujillo, R. Zucca, A. M. Van Loey, T. Grauwet and M. E. Hendrickx, In Vitro Digestibility Kinetics of Oil-in-Water Emulsions Structured by Water-Soluble Pectin-Protein Mixtures from Vegetable Purées, *Food Hydrocolloids*, 2018, **80**, 231–244, DOI: [10.1016/j.foodhyd.2018.02.007](https://doi.org/10.1016/j.foodhyd.2018.02.007).
- 59 M. Kurpiers, J. D. Wolf, C. Steinbring, S. Zaichik and A. Bernkop-Schnürch, Zeta Potential Changing Nanoemulsions Based on Phosphate Moiety Cleavage of a PEGylated Surfactant, *J. Mol. Liq.*, 2020, **316**, 113868, DOI: [10.1016/j.molliq.2020.113868](https://doi.org/10.1016/j.molliq.2020.113868).
- 60 L. Salvia-Trujillo, A. Rojas-Graü, R. Soliva-Fortuny and O. Martín-Belloso, Physicochemical Characterization and Antimicrobial Activity of Food-Grade Emulsions and Nanoemulsions Incorporating Essential Oils, *Food Hydrocolloids*, 2015, **43**, 547–556, DOI: [10.1016/j.foodhyd.2014.07.012](https://doi.org/10.1016/j.foodhyd.2014.07.012).



- 61 A. Molet-Rodríguez, A. Turmo-Ibarz, L. Salvia-Trujillo and O. Martín-Belloso, Incorporation of Antimicrobial Nanoemulsions into Complex Foods: A Case Study in an Apple Juice-Based Beverage, *LWT – Food Sci. Technol.*, 2021, **141**, 110926, DOI: [10.1016/j.lwt.2021.110926](https://doi.org/10.1016/j.lwt.2021.110926).
- 62 J. S. J. Santiago, L. Salvia-Trujillo, A. Palomo, A. Niroula, F. Xu, A. M. Van Loey and M. E. Hendrickx, Process-Induced Water-Soluble Biopolymers from Broccoli and Tomato Purées: Their Molecular Structure in Relation to Their Emulsion Stabilizing Capacity, *Food Hydrocolloids*, 2018, **81**, 312–327, DOI: [10.1016/j.foodhyd.2018.03.005](https://doi.org/10.1016/j.foodhyd.2018.03.005).
- 63 D. Fu, S. Deng, D. J. McClements, L. Zhou, L. Zou, J. Yi, C. Liu and W. Liu, Encapsulation of β -Carotene in Wheat Gluten Nanoparticle-Xanthan Gum-Stabilized Pickering Emulsions: Enhancement of Carotenoid Stability and Bioaccessibility, *Food Hydrocolloids*, 2019, **89**, 80–89, DOI: [10.1016/j.foodhyd.2018.10.032](https://doi.org/10.1016/j.foodhyd.2018.10.032).
- 64 S. Finnie and W. A. Atwell, *Wheat Flour*, AACC International Handbook Series, Second Edition., 2016.
- 65 R. C. Hoseney, Dough Forming Properties, *J. Am. Oil Chem. Soc.*, 1979, **56**(1), A78–A81, DOI: [10.1007/BF02671788](https://doi.org/10.1007/BF02671788).
- 66 F. Cabrera-Chávez, J. M. Ezquerro-Brauer, R. Herrera-Urbina, C. M. Rosell and O. Rouzaud-Sáñez, Physicochemical Properties of Wheat Gluten Proteins Modified by Protease from Sierra (*Scomberomorus* Sierra), Fish, *Int. J. Food Prop.*, 2010, **13**(6), 1187–1198, DOI: [10.1080/10942910903013357](https://doi.org/10.1080/10942910903013357).
- 67 A. C. de Aguiar, J. T. de Paula, J. L. M. Mundo, J. Martínez and D. J. McClements, Influence of Type of Natural Emulsifier and Microfluidization Conditions on Capsicum Oleoresin Nanoemulsions Properties and Stability., *J. Food Process Eng.*, 2021, **44**(4), e13660, DOI: [10.1111/jfpe.13660](https://doi.org/10.1111/jfpe.13660).
- 68 Y. Q. Zhu, X. Chen, D. J. McClements, L. Zou and W. Liu, Pickering-Stabilized Emulsion Gels Fabricated from Wheat Protein Nanoparticles: Effect of PH, NaCl and Oil Content, *J. Dispers. Sci. Technol.*, 2018, **39**(6), 826–835, DOI: [10.1080/01932691.2017.1398660](https://doi.org/10.1080/01932691.2017.1398660).
- 69 R. Pal, Effect of Droplet Size on the Rheology of Emulsions, *AIChE J.*, 1996, **42**(11), 3181–3190, DOI: [10.1002/aic.690421119](https://doi.org/10.1002/aic.690421119).
- 70 M. Pierre, Y. Piemi, D. Korner, S. Benita and J.-P. Marty, Positively and Negatively Charged Submicron Emulsions for Enhanced Topical Delivery of Antifungal Drugs, *J. Controlled Release*, 1999, **58**(2), 177–187, DOI: [10.1016/S0168-3659\(98\)00156-4](https://doi.org/10.1016/S0168-3659(98)00156-4).
- 71 S. Hoeller, A. Sperger and C. Valenta, Lecithin Based Nanoemulsions: A Comparative Study of the Influence of Non-Ionic Surfactants and the Cationic Phytosphingosine on Physicochemical Behaviour and Skin Permeation, *Int. J. Pharm.*, 2009, **370**(1–2), 181–186, DOI: [10.1016/j.ijpharm.2008.11.014](https://doi.org/10.1016/j.ijpharm.2008.11.014).
- 72 J. Jiang, J. Chen and Y. L. Xiong, Structural and Emulsifying Properties of Soy Protein Isolate Subjected to Acid and Alkaline PH-Shifting Processes, *J. Agric. Food Chem.*, 2009, **57**(16), 7576–7583, DOI: [10.1021/jf901585n](https://doi.org/10.1021/jf901585n).
- 73 J. Wu, F. Xu, Y. Wu, W. Xiong, M. Pan, N. Zhang, Q. Zhou, S. Wang, X. Ju and L. Wang, Characterization and Analysis of an Oil-in-Water Emulsion Stabilized by Rapeseed Protein Isolate under PH and Ionic Stress, *J. Sci. Food Agric.*, 2020, **100**(13), 4734–4744, DOI: [10.1002/jsfa.10532](https://doi.org/10.1002/jsfa.10532).
- 74 Y. H. Hong and D. J. McClements, Modulation of PH Sensitivity of Surface Charge and Aggregation Stability of Protein-Coated Lipid Droplets by Chitosan Addition, *Food Biophys.*, 2007, **2**(1), 46–55, DOI: [10.1007/s11483-007-9028-5](https://doi.org/10.1007/s11483-007-9028-5).
- 75 T. Rahaman, T. Vasiljevic and L. Ramchandran, Shear, Heat and PH Induced Conformational Changes of Wheat Gluten - Impact on Antigenicity, *Food Chem.*, 2016, **196**, 180–188, DOI: [10.1016/j.foodchem.2015.09.041](https://doi.org/10.1016/j.foodchem.2015.09.041).
- 76 W. Alencar-Luciano, M. Magnani, O. Martín-Belloso and L. Salvia-Trujillo, Effect of Digestible versus Non-Digestible Citral Nanoemulsions on Human Gut Microorganisms: An in Vitro Digestion Study, *Food Res. Int.*, 2023, **173**, 113313, DOI: [10.1016/j.foodres.2023.113313](https://doi.org/10.1016/j.foodres.2023.113313).
- 77 H. Cui, Q. Liu, D. J. McClements, B. Li, S. Liu and Y. Li, Development of Salt-and Gastric-Resistant Whey Protein Isolate Stabilized Emulsions in the Presence of Cinnamaldehyde and Application in Salad Dressing, *Foods*, 2021, **10**(8), 1868, DOI: [10.3390/foods10081868](https://doi.org/10.3390/foods10081868).
- 78 C. Ma, S. Xia, J. Song, Y. Hou, T. Hao, S. Shen, K. Li, C. Xue and X. Jiang, Yeast Protein as a Novel Dietary Protein Source: Comparison with Four Common Plant Proteins in Physicochemical Properties, *Curr. Res. Food Sci.*, 2023, **7**, 100555, DOI: [10.1016/j.crfs.2023.100555](https://doi.org/10.1016/j.crfs.2023.100555).
- 79 A. Brodkorb, L. Egger, M. Alminger, P. Alvito, R. Assunção, S. Ballance, T. Bohn, C. Bourlieu-Lacanal, R. Boutrou, F. Carrière, A. Clemente, M. Corredig, D. Dupont, C. Dufour, C. Edwards, M. Golding, S. Karakaya, B. Kirkhus, S. Le Feunteun, U. Lesmes, A. Macierzanka, A. R. Mackie, C. Martins, S. Marze, D. J. McClements, O. Ménard, M. Minekus, R. Portmann, C. N. Santos, I. Souchon, R. P. Singh, G. E. Vegarud, M. S. J. Wickham, W. Weitschies and I. Recio, INFOGEST Static in Vitro Simulation of Gastrointestinal Food Digestion, *J. Nat. Protoc.*, 2019, **14**(4), 991–1014, DOI: [10.1038/s41596-018-0119-1](https://doi.org/10.1038/s41596-018-0119-1).
- 80 T. Bohn, G. J. Mcdougall, A. Alegría, M. Alminger, E. Arrigoni, A. M. Aura, C. Brito, A. Cilla, S. N. El, S. Karakaya, M. C. Martínez-Cuesta and C. N. Santos, Mind the Gap-Deficits in Our Knowledge of Aspects Impacting the Bioavailability of Phytochemicals and Their Metabolites-a Position Paper Focusing on Carotenoids and Polyphenols, *Mol. Nutr. Food Res.*, 2015, **59**(7), 1307–1323, DOI: [10.1002/mnfr.201400745](https://doi.org/10.1002/mnfr.201400745).
- 81 C. Zhang, W. Xu, W. Jin, B. R. Shah, Y. Li and B. Li, Influence of Anionic Alginate and Cationic Chitosan on Physicochemical Stability and Carotenoids Bioaccessibility of Soy Protein Isolate-Stabilized Emulsions, *Food Res. Int.*, 2015, **77**, 419–425, DOI: [10.1016/j.foodres.2015.09.020](https://doi.org/10.1016/j.foodres.2015.09.020).
- 82 T. Tokle, Y. Mao and D. J. McClements, Potential Biological Fate of Emulsion-Based Delivery Systems: Lipid Particles Nanolaminated with Lactoferrin and β -Lactoglobulin



- Coatings, *Pharm. Res.*, 2013, **30**(12), 3200–3213, DOI: [10.1007/s11095-013-1003-x](https://doi.org/10.1007/s11095-013-1003-x).
- 83 K. Ahmed, Y. Li, D. J. McClements and H. Xiao, Nanoemulsion- and Emulsion-Based Delivery Systems for Curcumin: Encapsulation and Release Properties, *Food Chem.*, 2012, **132**(2), 799–807, DOI: [10.1016/j.foodchem.2011.11.039](https://doi.org/10.1016/j.foodchem.2011.11.039).
- 84 H. D. Silva, J. Poejo, A. C. Pinheiro, F. Donsi, A. T. Serra, C. M. M. Duarte, G. Ferrari, M. A. Cerqueira and A. A. Vicente, Evaluating the Behaviour of Curcumin Nanoemulsions and Multilayer Nanoemulsions during Dynamic in Vitro Digestion, *J. Funct. Foods*, 2018, **48**, 605–613, DOI: [10.1016/j.jff.2018.08.002](https://doi.org/10.1016/j.jff.2018.08.002).
- 85 A. Gasa-Falcon, A. Acevedo-Fani, G. Oms-Oliu, I. Odriozola-Serrano and O. Martín-Belloso, Development, Physical Stability and Bioaccessibility of β -Carotene-Enriched Tertiary Emulsions, *J. Funct. Foods*, 2020, **64**, 103615, DOI: [10.1016/j.jff.2019.103615](https://doi.org/10.1016/j.jff.2019.103615).
- 86 A. C. Pinheiro, M. A. Coimbra and A. A. Vicente, In Vitro Behaviour of Curcumin Nanoemulsions Stabilized by Biopolymer Emulsifiers - Effect of Interfacial Composition, *Food Hydrocolloids*, 2016, **52**, 460–467, DOI: [10.1016/j.foodhyd.2015.07.025](https://doi.org/10.1016/j.foodhyd.2015.07.025).
- 87 Y. Reynaud, M. Lopez, A. Riaublanc, I. Souchon and D. Dupont, Hydrolysis of Plant Proteins at the Molecular and Supra-Molecular Scales during in Vitro Digestion, *Food Res. Int.*, 2020, **134**, 109204, DOI: [10.1016/j.foodres.2020.109204](https://doi.org/10.1016/j.foodres.2020.109204).
- 88 C. Soukoulis, S. Cambier, L. Hoffmann and T. Bohn, Chemical Stability and Bioaccessibility of β -Carotene Encapsulated in Sodium Alginate o/w Emulsions: Impact of Ca²⁺ Mediated Gelation, *Food Hydrocolloids*, 2016, **57**, 301–310, DOI: [10.1016/j.foodhyd.2016.02.001](https://doi.org/10.1016/j.foodhyd.2016.02.001).
- 89 M. Iddir, C. Degerli, G. Dingo, C. Desmarchelier, T. Schlee, P. Borel, Y. Larondelle and T. Bohn, Whey Protein Isolate Modulates Beta-Carotene Bioaccessibility Depending on Gastro-Intestinal Digestion Conditions, *Food Chem.*, 2019, **291**, 157–166, DOI: [10.1016/j.foodchem.2019.04.003](https://doi.org/10.1016/j.foodchem.2019.04.003).
- 90 M. Ramezani, M. Amengual Ramon, L. Salvia-Trujillo and O. Martín-Belloso, Replication Data for: Plant-Protein Stabilized Emulsions as β -Carotene Delivery Systems: Colloidal Stability and Behaviour during in Vitro Digestion Conditions, *CORA.Repositori de Dades de Recerca*, 2025, **1**, DOI: [10.34810/data2788](https://doi.org/10.34810/data2788).

